EVOLUTION OF AN INFINITESIMAL THREE-DIMENSIONAL DISTURBANCE IN AN INVISCID PARALLEL SHEAR FLOW NEAR A WALL

By

Pierre Jean Reboul
Dipl. Eng., National Polytechnical Institute of Grenoble, France, 1992

Submitted to the Department of Aeronautics and Astronautics
in partial fulfillment of the requirements for the degree of

Master of Science in Aeronautics and Astronautics
at the
Massachusetts Institute of Technology

February 1993

Author..... .....
Department of Aeronautics and Astronautics
October 19, 1992

Certified by.....
Marten T. Landahl
Professor of Aeronautics and Astronautics
Thesis Supervisor

Accepted by..... .....
Professor Harold Y. Wachman
Chairman, Departmental Graduate Committee

Evolution of an infinitesimal three-dimensional disturbance in an inviscid parallel shear flow near a wall

by

Pierre Jean Reboul

Submitted to the Department of Aeronautics and Astronautics
on October 20, 1992, in partial fulfillment of the
requirements for the degree of
Master of Science in Aeronautics and Astronautics

Abstract

The near wall turbulence structure in a boundary layer is characterized by streamwise streaks of low and high speed regions. A simplified model is given in which the interaction of a localized initial disturbance with the mean shear U is emphasized as the fundamental process. The evolution of this infinitesimal three dimensional disturbance is studied on the basis that, for fairly long times, nonlinearities have not the time to act, which leads to an inviscid and linear treatment. A first order approximation of the vertical component of the fluctuating velocity v is used as well. The liftup of a fluid element is found to be stretched over time with its corresponding v decreasing as $\frac{1}{t}$. For inflectional profiles, the model suggests that a growth in v could occur for profiles having a large positive U" below the inflection point.

Thesis Supervisor: Marten T. Landahl
Title: Professor of Aeronautics and Astronautics

Acknowledgments

I would like to express my thanks to my research advisor, Pr M.T. Landahl, for having allowed me to work on this interesting topic, and under his guidance.

I would like to express my gratitude to Pr K. Breuer. His experience and hints were particularly helpful in the numerical phase of my research.

Pr A. Rowe, for whom I work two years at the Institute of Mechanics of Grenoble, France, taught me Computational Fluid Dynamics. I shall never forget his friendship, and I am indebted to him.

I would like to thank Pr M.Lesieur and Pr R.Moreau from the School of Hydraulics and Mechanics, Grenoble, France. They taught me most of the Fluid Mechanics I know.

I also would like to dedicate this thesis to my parents and siblings who supported me both financially and morally all along this year.

Finally, I have to express my infinite appreciation to Violaine. Without her emotional support this work would not have been possible.

Contents

1 Introduction **9**

1.1 Transition to turbulence 9

1.1.1 Transition process 9

1.1.2 Sublayer streaks 11

1.2 Hydrodynamical instability 12

1.2.1 Reminder of the linear instability theory 12

1.2.2 Treatment of 3D disturbances, Algebraic instability 13

1.3 Modelling 14

2 Governing Equations **16**

2.1 Basic formulation 16

2.2 Initial value problem 19

2.3 Integral formulation 20

2.3.1 Derivation of the vertical velocity component v 20

2.3.2 Derivation of the liftup 22

3 Long time behavior of the flow **24**

3.1 Liftup equation 24

3.1.1 Description of the equation 24

3.1.2 Simplifications 25

3.2 Stable case 27

3.3 Unstable case 29

3.3.1 Liftup equation for large U" 29

3.3.2 Comparison with the linear stability theory 30

4 Numerical model **31**

4.1 Numerical scheme 31

4.1.1 Discretization 31

4.1.2 Grid 32

4.2 Inputs 33

4.2.1 U profiles 33

4.2.2 Initial disturbance 34

4.2.3 Timestep and spacestep 35

4.3 Outputs 36

5 Results **37**

5.1 Couette flow 37

5.2 Stable profiles 41

5.2.1 Liftup 41

5.2.2 Vertical component of the fluctuating velocity v 43

5.3 Unstable profiles 47

5.3.1 Study of the U"-dependent term 47

5.3.2 Evolution of the liftup for a large U" 51

6 Conclusions **55**

A Why the liftup cannot be a function of ξ alone **57**

B An alternative equation for the liftup **59**

C Mean flow profiles and initial disturbances **61**

List of Figures

1-1 Idealized sketch of the transition process on a flat plate 10

1-2 Top view of the near wall structure of a turbulent flat-plate boundary layer, visualized with hydrogen bubbles. 11

1-3 Conceptual burst model: (a) Mechanics of streak formation, (b) mechanics of streak breakup. 12

2-1 Coordinate system, definitions. 17

3-1 Mean velocity profiles: (a) Stable, (b) Couette flow, (c) Unstable . . . 27

4-1 Computation Grid 33

5-1 Liftup and comparison between $v_{computed}$ (.) and v_{exact} (+) for t=50 and 100. Δx =10, Δt =1, y=0.1 39

5-2 Evolution of the liftup over time, t=20 (continuous), 50 (-), 100 (.). Δx =50, Δy =0.1, Δt =1, y=0.5 40

5-3 Evolution of v over time, t=20 (continuous), 50 (-), 100 (.). Δx =50, Δy =0.1, Δt =1, y=0.5 40

5-4 Evolution of l over time, t=50 (continuous), 100 (o), 150 (+), 200 (*). Δx =10, Δt =1, y=0.1, Λ =1 42

5-5 Evolution of $\bar{l}$ for the symmetrical (+) and asymmetrical (*) disturbances. Δx =10, Δt =1, y=0.1, Λ =1 43

5-6 Evolution of v over time, t=50 (continuous), 100 (o), 150 (+), 200 (*). Δx =10, Δt =1, y=0.1, Λ =1 45

5-7 Evolution of $\bar{v}$ for the symmetrical (+) and asymmetrical (*) disturbances. Δx =10, Δt =1, y=0.1, Λ =1 46
5-8 Evolution of v(x=0, y=0.1) with time. Δt = 1, Λ =1 46
5-9 v(x=0, y=0.1)t vs time. Δt =1, y=0.1, Λ =1 47
5-10 Difference of evolution of the liftup and v with x for a symmetrical ((a) and (b)) and an asymmetrical disturbance ((c) and (d)). Δx =10, Δt =1, y=0.1, Λ =1, t=200. 48
5-11 Contribution of the U"-dependent term to the liftup for the stable and the unstable case. Δx =10, Δt =1, y=0.1, Λ =1 and -10, t=50 . . . 50
5-12 Temporal growth rate of the U"-dependent term. Δx =10, Δt =1, y=0.1, Λ =1 (-) and -10 (continuous), t=50 51
5-13 Contribution of the U"-dependent term to the liftup for a profile having a large U"at y=0.1. Δx =10, Δt =1, y=0.1, U"(0.1)=95, t=10 and 20. Figures (b) and (d): G_0 (continuous), liftup (-) 53
5-14 Contribution of the U"-dependent term to the liftup for a profile having a large U"at y=0.1. Δx =10, Δt =1, y=0.1, U"(0.1)=95, t=30. Bottom figure: G_0 (continuous), liftup (-) 54

C-1 Karman-Polhausen profiles: Stable Blasius profile Λ =1 (continuous), unstable profile (+) Λ =-10, separation profile (o) Λ =-12 62
C-2 ϕ_0 for a symmetrical (continuous) and an asymmetrical disturbance (-), L_x=200, L_y=1, y=0.1 62
C-3 Global shape of ϕ_0 for a symmetrical and an asymmetrical disturbance, L_x=200, L_y=1 63

Nomenclature

- U(y): mean stremwise velocity
- U'(y): derivative of U with respect to y
- U"(y): second derivative of U with respect to y
- μ: dynamic viscosity
- ρ: density
- $\nu = \frac{\mu}{\rho}$: kinematic viscosity
- $Re = \frac{Ux}{\nu}$: Reynolds number
- x: streamwise distance from the leading edge of the flat plate
- δ: boundary layer thickness
- $u^* = \nu \left(\frac{dU}{dy}\right)_{y=0}$: friction velocity
- $y^+ = \frac{yu^*}{\nu}$: vertical wall unit
- u: streamwise fluctuating velocity
- v: vertical fluctuating velocity
- p: total pressure
- τ_{ij}: Reynolds stresses
- Λ: Karman-Polhausen parameter
- Δx: spacestep in x
- Δt: timestep in t

Chapter 1

Introduction

1.1 Transition to turbulence

Transition to turbulence has been extensively studied by researchers in fluid mechanics but after, now, more than 90 years of research on the transition process, we can still present only a an incomplete description. The linear stability theory predicts the demise of laminar flow at some finite Reynolds number, but does not predict the onset of turbulence [12]. Following the initial growth of infinitesimal wave-like disturbances, the flow passes through a complicated sequence of spatial and temporal changes; the end result is that unsteady and disorderly but rational and statistically stable phenomenon known as turbulence. The whole process of change from laminar to turbulent flow is termed transition. (See Figure 1-1)

1.1.1 Transition process

In practice, the transition to turbulence in a boundary layer over a semi-infinite flat plate proceeds as follows (See Lesieur, 1991) [6]. The layer is first laminar up to a Reynold's number around 100000; then two-dimensional Tollmien-Schlichtling waves, (T-S waves) begin to grow. Thereafter, experiments show the development of a span-wise oscillation of the wave, interpreted as the evidence of the initiation of a hairpin-shaped vortex structure in the boundary layer. The regions of high fluctuations, the

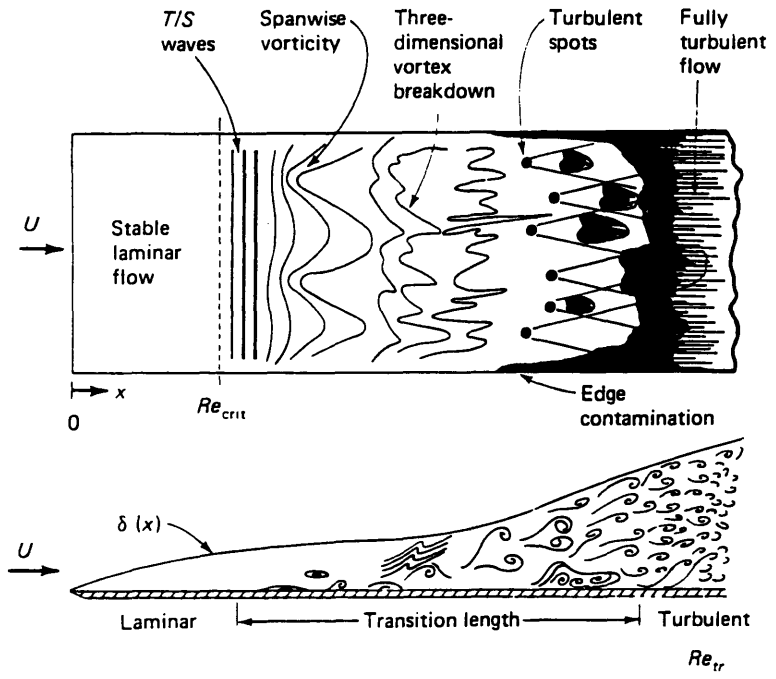

Figure 1-1: Idealized sketch of the transition process on a flat plate

so-called peaks, are characterized by high longitudinal velocity fluctuations, while the valleys correspond to low fluctuations. One observes the formation of longitudinal streaks, which we will examine later on, of respectively slow and high-speed flows in the peaks and the valleys. The formation of these streaks could be understood by noticing that longitudinal vortices of opposite vorticity on each side of a peak will pump slow fluid from the wall. The hairpin vortex is then strained downstream, and the longitudinal velocity profile becomes inflectional in the peak. All these longitudinal and spanwise inflectional instabilities contribute to the roll-up and breakdown of T-S waves into three-dimensional turbulence. In a naturally developing boundary layer, transition is intermittent in the sense that the above-described process occurs in turbulent spots which are spatially localized. For Re greater than 1,000,000, the boundary layer is turbulent everywhere. In the present thesis we are particularly interested in the formation of these streamwise streaks.

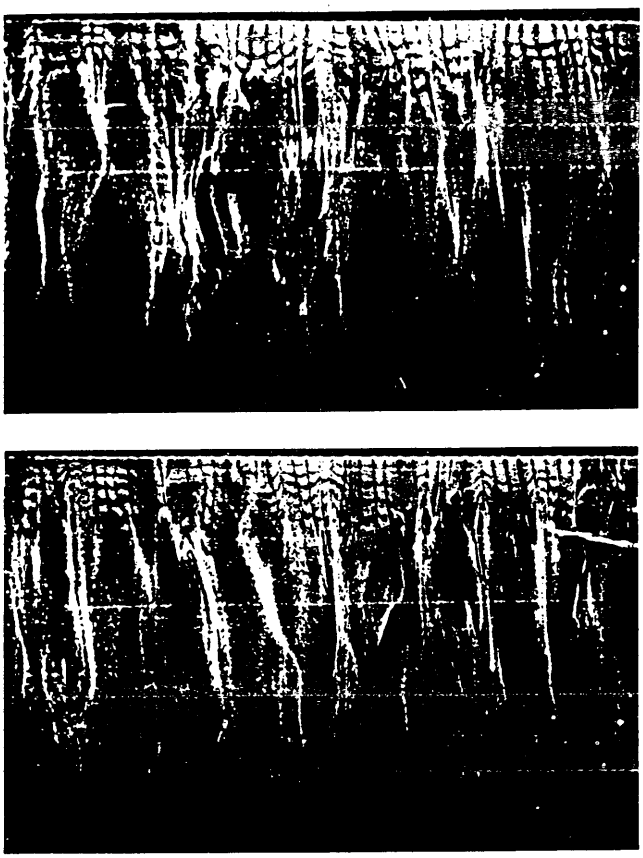

Figure 1-2: Top view of the near wall structure of a turbulent flat-plate boundary layer, visualized with hydrogen bubbles.

1.1.2 Sublayer streaks

These so-called sublayer streaks were first brought out by the experiments performed by Kline and his group (1967) [11] and by Corino and Brodkey (1969) (See Figure 1-2). Using visualisation experiments, they detected bursting events in the near-wall region (in the viscous and buffer layers) separated by periods of unsteady laminar motion. These events gave birth to low and high-speed streaks which appeared as the predominant structure in this region. They also observed a typical regular spanwise spacing of about 100 in viscous wall-unit. The oscillation and lift-up of a low-speed streak was seen to initiate a rapid outflow of fluid from the wall-region and a subsequent breakup of the streak. Kline et al. (1967) proposed a conceptual model for this strongly intermittent bursting shown in Figure 1-3.

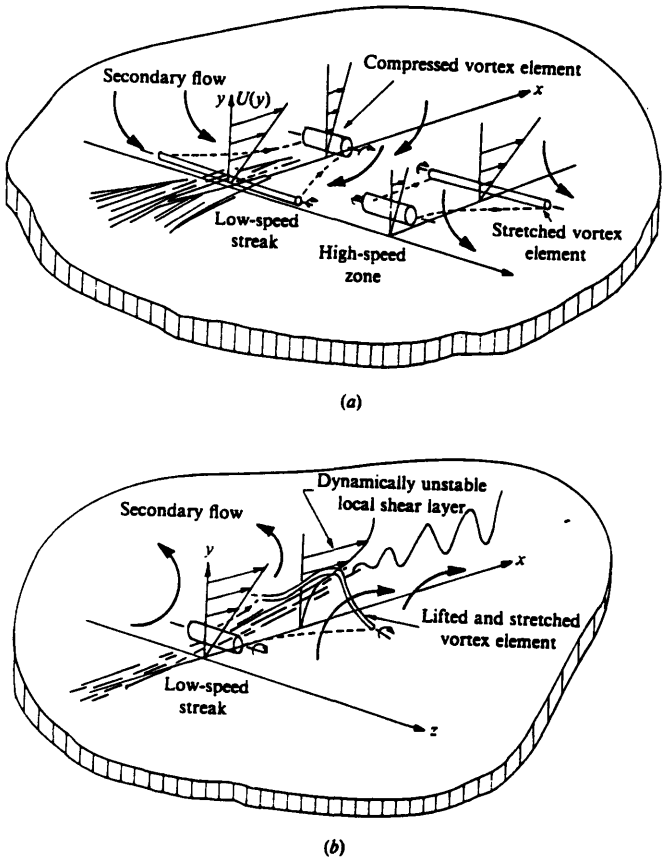

Figure 1-3: Conceptual burst model: (a) Mechanics of streak formation, (b) mechanics of streak breakup.

In view of the aim to find a suitable model of the near-wall turbulence, it is essential to understand how this strong intermittent phenomenon can arise. The linear hydrodynamic instability theory gives only a limited guidance as a non-inflectional mean velocity profile for a flat-plate boundary layer is inviscidly stable to wave trains of infinitesimal amplitude. But this theory is based on the examination of infinite sinusoidal wave trains which may exclude an important class of disturbances, as it will become apparent later.

1.2 Hydrodynamical instability

1.2.1 Reminder of the linear instability theory

The question of under what conditions a parallel shear flow will become unstable has been one of the central problems in hydrodynamic research since the finding by Rayleigh (1880) that a necessary condition for a parallel inviscid shear flow to have

wavelike disturbances growing exponentially with time is that the velocity profile possesses an inflection point. Tolllmien (1929) showed that this necessary condition is also sufficient for wall-bounded flows. Fjortoft (1950) later showed that this inflection point must correspond to a maximum shear. Arnold's (1965) demonstrated that Rayleigh's criterion also holds for finite disturbances. Such results are useful for understanding the global stability of a disturbance in form of an infinite wave train. However, the evolution in space and in time of an arbitrary three-dimensional disturbance is less well understood.

1.2.2 Treatment of 3D disturbances, Algebraic instability

This problem was first addressed by Orr (1907) [9], but only a few researchers came out with significant results. Wilke (1967) [13] carried out a study of the asymptotic behavior of infinitesimal three-dimensional disturbances, for large times. He showed that for initial disturbances independent of the streamwise direction, the perturbation kinetic energy may reach values up to twice the kinetic energy of the unperturbed flow. Later, Ellingsen and Palm (1975) [1] demonstrated that a streamwise perturbation velocity increasing linearly with time will result. This issue was also addressed by Landahl (1980) [2]. He showed that an inviscid parallel flow may suffer algebraic type instability with the total perturbation energy growing at least as fast as t for a three dimensional initial perturbation having a non-zero vertical momentum. The streamwise momentum and perturbation energy growth manifests itself through a continuous increase of the perturbed region with a strea mwise perturbation velocity tending to a finite value in a Lagrangian frame of reference. This type of instability may arise in any inviscid shear flow, whether stable or unstable in the Rayleigh sense. In case of an inflectional profile, of course, this algebraic growth is overcome by an exponential one which dominates for large times and gives rise to an instability.

That the simple linearized inviscid theory indicates this behavior may be related to the appearance of the longitudinal streaks described earlier on.

1.3 Modelling

Now that we have seen the relationship between hydrodynamical instabilities and the near wall turbulence (e.g the formation of streaks), we shall acknowledge the advantages of a new formulation in order to model these streaks.

Several models including this algebraic instability concept have been developed. Two models are particularly interesting since they avoid the difficulty to deal with nonlinear equations. A brief review of these models is given below.

The first approach is to assume the nonlinearity to serve as an intermittent disturbance source localized in the near-wall region, with the remainder of the flow responding in a linear fashion to this random fluctuation source, in the spirit of Lighthill's theory for aerodynamic noise (See Landahl, 1992) [3]. This means that one has to solve a linear system forced by intermittent nonlinearities.

The second approach consists in breaking up the flow in three appropriate time scales (e.g linear, viscous and nonlinear) (See Landahl, 1992) [4]. The main advantage of this approach is that the early linear stage (or shear interaction stage), during which nonlinearities have not time to act, provides the initial conditions for the later stages and simplify considerably their treatment. Besides, the new trend is to use an integral approach that involves the liftup of the fluid element also appearing in Prandtl's mixing length theory [10]. This formulation is particularly useful for the study of the zero streamwise wave number component, and, above all, avoids to get into a spectral analysis of the initial disturbance.

These two models agree on the conclusion that for short times after creation of the flow structure, the effect of viscosity may be neglected. Using an inviscid model, corresponding to the first stage of the second model, we expect in this thesis to be

able to see most of the flow features described earlier, on the assumption that the model remains applicable for fairly long evolutionary times. Thus we are going to study the evolution of an infinitesimal three-dimensional disturbance, in the inviscid case, using an integral formulation. We look for the relationship of the now theory with the classical Rayleigh's approach. Especially, we want to make sure to find, for large times, a growth in the perturbation velocity component perpendicular to the wall, in the case of an inflectional profile. In order to validate the model, we should also find for a stable profile, this component to decrease as $1/t$ as well as the main features of the algebraic instability.

Chapter 2 describes the governing equations.

Chapter 2

Governing Equations

2.1 Basic formulation

In the following formulation, we consider a parallel mean shear flow U(y), on which a three-dimensional disturbance is superimposed.

Notation: (See Figure 2-1)

- $U(x_2)$ is the mean velocity (where $x_2 = y$)
- $u_i(x_j, t)$ are the fluctuating velocities.
- p is the total pressure.
- δ is Kronecker's symbol

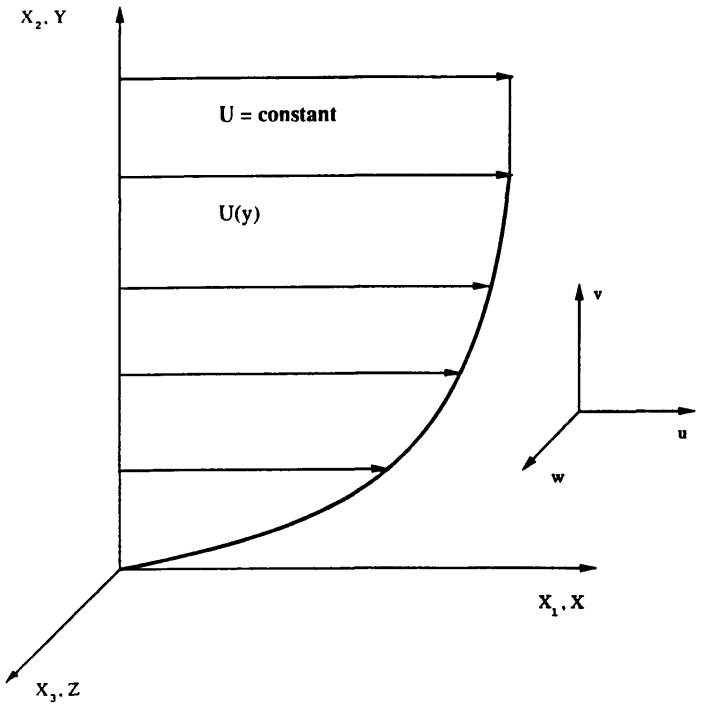

Figure 2-1: Coordinate system, definitions.

The Navier-Stokes equations give the following set of equations for the fluctuating field:

$$\frac{Du_i}{Dt} + u_2 U'(x_2)\delta_{1i} = -\frac{1}{\rho}\frac{\partial p}{\partial x_i} + \frac{1}{\rho}\frac{\partial}{\partial x_j}[\mu\frac{\partial u_i}{\partial x_j} + \tau_{ij}] \tag{2.1}$$

where

$$\frac{D}{Dt} \equiv \frac{\partial}{\partial t} + U\frac{\partial}{\partial x_1} \tag{2.2}$$

$$U' \equiv \frac{dU}{dx_2} \tag{2.3}$$

and where

$$\tau_{ij} = -\rho(u_i u_j - \overline{u_i u_j}) \tag{2.4}$$

are the "fluctuating Reynolds stresses", the overbar denoting averaged values.

The equations (2.2) and (2.5) have been obtained by subtraction of the equations for the mean flow from the full set of equations. The velocity field is submitted to the following initial and boundary conditions.

- Initial conditions (t=0):

$$u_1 = u = u_0, u_2 = v = v_0, u_3 = w = w_0$$

- Boundary conditions: All velocities have to vanish at y=0 and y=∞ The disturbance field is assumed to be horizontally localized so that the disturbance velocities and the perturbation pressure decay at large x and z.

Elimination of the pressure p using the continuity equation

$$\frac{\partial u_i}{\partial x_i} = 0 \tag{2.5}$$

gives the following equation for the vertical component of the velocity (perpendicular to the wall):

$$\frac{D\nabla^2 v}{Dt} - \frac{\partial v}{\partial x} U'' - \nu \nabla^4 v = q, \tag{2.6}$$

where

$$\nabla^2 \equiv \frac{\partial^2}{\partial x^2} + \frac{\partial^2}{\partial y^2} + \frac{\partial^2}{\partial z^2} \tag{2.7}$$

$$q = \nabla^2 T_2 - \frac{\partial^2 T_i}{\partial x_i \partial x_j}, \tag{2.8}$$

$$T_i = \frac{1}{\rho} \frac{\partial \tau_{ij}}{\partial x_j} \tag{2.9}$$

Of course for infinitesimal amplitudes of v, one recovers the well-known Orr-Sommerfeld equation (in the physical space and not Fourier's space as usual).

2.2 Initial value problem

This well-known problem consists in solving Orr-Sommerfeld equation, with the boundary conditions described earlier.

In the present thesis the inviscid version of this equation, namely Rayleigh equation, will be treated:

Rayleigh equation is:

$$\frac{D\nabla^2 v}{Dt} = q + U''\frac{\partial v}{\partial x} \tag{2.10}$$

Using (2.6), it may be written as follow:

$$\frac{D\phi}{Dt} = q_1 \tag{2.11}$$

with

$$q_1 = q + U''\frac{\partial v}{\partial x} \tag{2.12}$$

$$\phi = \nabla^2 v \tag{2.13}$$

One can introduce the quantity l, "liftup" of a fluid element, defined by

$$l(x,y,z,t) = \int_0^t v Dt = \int_0^t v(\xi + U(y)t_1, y, z, t_1)dt_1 \tag{2.14}$$

As mentioned in the introduction, two methods have been developed to solve the initial value problem, and one can get a deeper insight considering equation (2.10). One can:

- Either regard the right-hand side of (2.10) as a given "source term", and treat the flow as a linear system forced in a random manner by the nonlinear interaction between the velocity components. Then, one can use an intermittency formulation, (see Landahl 1990) [4] pretending that nonlinearities act at $t{=}t_n{=}t_0$,

and set:

$$q = Q_n(x, y, z)\delta(t - t_n) \tag{2.15}$$

where δ is the Dirac function.

- Or we can break up the problem in three different time scales, namely, a shear interaction stage, a viscous one, and a nonlinear one. We solve for v at a time t, such as $t < t_s$, for which nonlinear effects have not had time to develop.

  $t_s = \frac{1}{U'(y=0)}$ (shear interaction time, see Landahl (1992) [5])

  And in that case, q = 0

In this thesis, the second approach, the more recent, will be covered. This corresponds to the inviscid and linear problem.

One can solve for ϕ right away.

$$\phi(x, y, z, t) = \int_{-\infty}^{t} q_1(\xi + U(y)t_1, y, z, t_1)dt_1 \tag{2.16}$$

where ξ = x - U(y)t.

This gives:

$$\phi(x, y, z, t) = \phi_0(\xi, y, z) + \frac{\partial l}{\partial x}U'' \tag{2.17}$$

Here ϕ_0 corresponds to the initial three-dimensional disturbance.

2.3 Integral formulation

2.3.1 Derivation of the vertical velocity component v

Knowing ϕ(x,y,z,t), it is easy to solve for v using the Poisson equation (2.12). We use a Fourier transform is the x,z-plane:

- ˜ denotes transformed quantities

- α and β are respectively the x and z transformed variables
- we set as usual k, by

$$k^2 = \alpha^2 + \beta^2$$

- ' denotes the derivative with respect to y

Equation (2.12) is transformed in :

$$\tilde{v''} - k^2\tilde{v} = \tilde{\phi} \tag{2.18}$$

which is easily integrated in:

$$\tilde{v} = -\frac{1}{2k}\int_0^\infty [exp(-k|y-y_1|) - exp(-k(y+y_1))]\tilde{\phi}(y_1)dy_1 \tag{2.19}$$

where we have to respect the following boundary conditions in the physical space:

- v(x,y=0,z,t) = 0
- v(x,y=∞,z,t) = 0

We can perform a second order Taylor development of $\tilde{v}$ for small y. This leads to:

$$\tilde{v} \simeq \frac{1}{2}\int_0^\infty [|y-y_1| - y - y_1]\tilde{\phi}(y_1)dy_1 + ky\int_0^\infty y_1\tilde{\phi}(y_1)dy_1 \tag{2.20}$$

This can be inverted:

$$v \simeq \frac{1}{2}\int_0^\infty [|y-y_1| - y - y_1]\phi(y_1)dy_1$$

$$+ y\nabla_h^2\int_0^\infty\int_{-\infty}^\infty\int_{-\infty}^\infty \frac{y_1\phi(x_1,y_1,z_1)}{\sqrt{(x-x_1)^2+(z-z_1)^2}}dx_1dy_1dz_1 \tag{2.21}$$

where

$$\nabla_h^2 \equiv \frac{\partial^2}{\partial x^2} + \frac{\partial^2}{\partial z^2}$$

To begin with, we shall only use the first term of equation (2.21) which corresponds to the first order approximation. Later in this paper we shall refer to the so-called

near-wall approximation, namely:

$$v = \int_0^\infty C(y, y_1)\phi(x, y_1, z, t)dy_1 \tag{2.22}$$

where

$$C(y, y_1) = \frac{1}{2}[|y - y_1| - y - y_1]$$

2.3.2 Derivation of the liftup

Now we aim at solving for l(x,y,z,t).

Using the equations (2.13) (2.16) and (2.21) (in the inviscid case), one can obtain:

$$l(x, y, z, t) = \int_0^\infty C(y, y_1)[\int_0^t [\phi_0[\xi + (U(y) - U(y_1))t_1, y_1, z] + U''(y_1)\frac{\partial l}{\partial x}]dt_1]dy_1 \tag{2.23}$$

One can get rid of the x-derivative of l by using the following change of variables:

$$x_1 = x - U(y)(t - t_1) - U(y_1)t_1$$

and

$$x_1(t_1 = t) = x - U(y_1)t = \xi_1 \tag{2.24}$$

$$x_1(t_1 = 0) = x - U(y)t = \xi \tag{2.25}$$

Finally we get the integral equation on which all this paper hinges:

$$l(x, y, z, t) = \int_0^\infty C(y, y_1)\frac{\varphi_0(\xi_1, y_1, z) - \varphi_0(\xi, y_1, z)}{U(y) - U(y_1)}dy_1$$

$$+ \int_0^\infty C(y, y_1)U''(y_1)\frac{l(\xi_1, y_1, z, t) - l(\xi, y_1, z, t)}{U(y) - U(y_1)}dy_1 \tag{2.26}$$

where

$$\varphi_0(x, y, z) = \int_{-\infty}^{x} \phi_0(x_1, y, z) dx_1 \tag{2.27}$$

Next chapter is going to describe how equation (2.25) can be solved.

Chapter 3

Long time behavior of the flow

3.1 Liftup equation

3.1.1 Description of the equation

Since we deal with a stability analysis of the flow, we introduce the following notation:

$$G_0 = \int_0^\infty C(y, y_1) \frac{\varphi_0(\xi_1, y_1, z) - \varphi_0(\xi, y_1, z)}{U(y) - U(y_1)} dy_1 \tag{3.1}$$

Where $G_0(x, y, z, t)$ corresponds to the U"-independent part of the liftup.

Therefore,

$$l(x, y, z, t) = G_0(x, y, z, t) + \int_0^\infty C(y, y_1) U''(y_1) \frac{l(\xi_1, y_1, z, t) - l(\xi, y_1, z, t)}{U(y) - U(y_1)} dy_1 \tag{3.2}$$

This equation induces some interesting initial and boundary conditions:

- Initial condition: l(x,y,z,0) = l_0(x,y,z)
- Boundary conditions: l(-∞,y,z,t) = 0, l(∞,y,z,t) = l_∞ = cst

As we already mentioned, this equation is an implicit equation in l. This integral equation cannot be classified under a "well-known" type of integral equations since the second term exhibits two integrals containing the unknown function l(x,y,z,t). We

shall show later how it can be simplified without loosing the impact of U". An other interesting feature of equation (3.2) is that both terms contain Cauchy's principal value integrals. Indeed, they are both singular for y = y_1 which means that they converge only if the singularity is skipped in an appropriate manner. Namely, y_1 varies from 0 to y - ϵ and from y + ϵ to ∞. Where ϵ is much smaller than 1.

Our main interest in this thesis is to prove the formulation that led to the initial value problem to be in good agreement with the classical hydrodynamical instability theory. Especially, we aim at retrieving the main features of the flow for large times.

3.1.2 Simplifications

Several attempts of simplification of (3.2) have been performed. These were meant to give an explicit expression of the liftup. Unfortunately, none of them gave satisfactory results. These simplified analitycal expressions of the liftup are given in appendix along with their flaws. Because of the unrealistic features of these models we decided to implement a numerical model of (3.2). In view of creating a numerical solver of equation (3.2), it is interesting to simplify it so that it does not require too much computer time and memory. Especially, the long time behavior of the computed quantities demands a large number of iterations over t, provided the timestep is small for accuracy reasons. Moreover, if the mean flow profile presents large variations with y, or if one wants to capture the inflection points of an unstable profile, the spacestep in y has to be small too. Consequently, the aim is to alter equation (3.2) in order to use y only as a parameter. The following set of remarks allows to establish the parametric y-dependence of the involved integrals.

Using equations (2.27) and (2.28), we replace y_1 by ξ_1 in (3.2), keeping in mind that:

$$U(y = 0) = 0$$

$$U(y = \infty) = U_\infty$$

We get:

$$l(x,y,z,t) = G_0 + \int_{x-U_\infty t}^{x} C(y,y_1)\frac{U''(y_1)}{U'(y_1)}\frac{l(\xi,y_1) - l(\xi_1,y_1)}{\xi - \xi_1}d\xi_1$$

Moreover, we have:

$$\xi - \xi_1 = [U(y_1) - U(y)]t \tag{3.3}$$

Therefore, for large time and under the assumption that for $\xi - \xi_1$ has to remain finite, we can approximate:

$$y \simeq y_1$$

since the mean velocity is well-behaved. This induces:

$$C(y,y_1) \simeq -y$$

The new expression of the liftup is:

$$l(x,y,z,t) = -\frac{y}{U'(y)}\int_{x-U_\infty t}^{x}\frac{\varphi(\xi,y,z,t) - \varphi(\xi_1,y,z,t)}{\xi - \xi_1}d\xi_1$$

$$-\frac{yU''(y)}{U'(y)}\int_{x-U_\infty t}^{x}\frac{l(\xi,y,z,t) - l(\xi_1,y,z,t)}{\xi - \xi_1}d\xi_1 \tag{3.4}$$

The main advantage of this new expression is that it is easier to solve than (3.2). But now the contribution of the mean profile only appears in the three functions U(y), U'(y), and U"(y). Thus, one has to make sure that the loss of the entire profile does not affect the solution too much. The validity of this assumption will be checked out.

The liftup equation (3.2) is going to be solved for different kinds of mean flow profiles (See Figure 3-1).

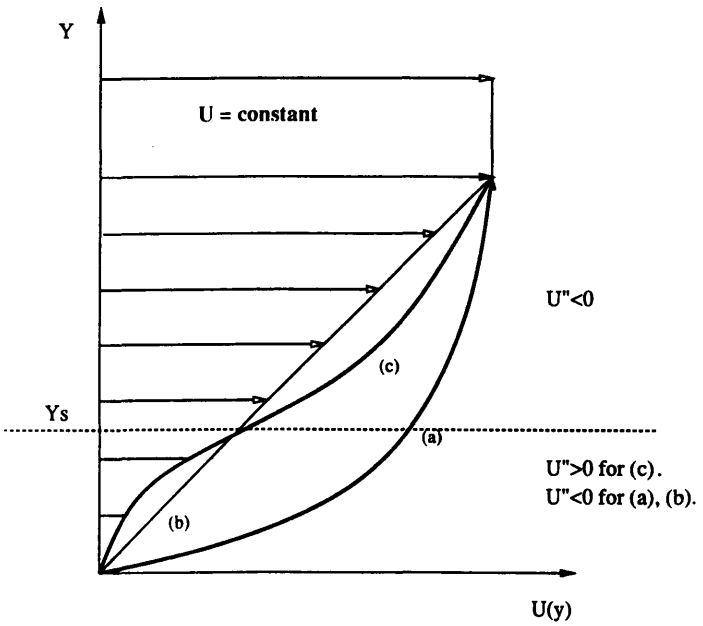

Figure 3-1: Mean velocity profiles: (a) Stable, (b) Couette flow, (c) Unstable

- Stable profile: U"$\geq$ 0, for y$\leq$ 0.
- Couette flow: U"=0, for all y.
- Inflectional profile: U"$\geq$0, for y$\leq Y_s$, where Y_s is the y-coordinate of the inflection point.

3.2 Stable case

In order to predict the stability of the flow, it is very important to assess the order of magnitude of each terms of equation (3.4). Landahl (1990) studied the evolution of the flow for a three-dimensional disturbance ϕ_0. He derived several relationships that are crucial for a global understanding of the flow behavior. Using streamwise averaging he obtained the following of equations.

The overbar denotes, now, the streamwise average, i.e:

$$\bar{l}(y,z,t) = \int_{-\infty}^{\infty} l(x,y,z,t)dx$$

- For a disturbance such as $\bar{\phi_0} \neq 0$:

$$\bar{v}(y,z,t) = \bar{v_0}(y,z) \tag{3.5}$$

$$\bar{u}(y,z,t) = \bar{u_0}(y,z) - tU'\bar{v_0}(y,z) \tag{3.6}$$

and

$$\bar{l}(y,z,t) = t\bar{v_0}(y,z) + \bar{l}_0 \tag{3.7}$$

- Of course if $\bar{\phi_0} = 0$, $\bar{v_0} = \frac{\partial^2 \bar{\phi_0}}{\partial y^2} = 0$, and

$$\bar{l} = \bar{v} = 0$$

$$\bar{u} = \bar{u_0}$$

These remarks will be particularly helpful when testing the numerical model. Indeed, they unveil the underlying mechanism of the algebraic instability. Equation (3.7) proves that the perturbed region grows linearly with time. This is consistent with the decay of v for large times. The v-component of the velocity does vanish but spreads its streamwise dimension.

One can go further and demonstrate that v decreases as fast as $\frac{1}{t}$ for large times. Starting with equation, and remembering that:

$$\frac{D}{Dt} = \left(\frac{\partial}{\partial t}\right)_{\xi=constant}$$

We have:

$$v = \left(\frac{\partial l}{\partial t}\right)_{\xi=constant}$$

$$v = -\frac{y}{U'(y)}\frac{[\varphi_0(x) - \varphi_0(x-t)]}{t} - \frac{yU''(y)}{U'(y)}\frac{[l(x,t) - l(x-t,t)]}{t}$$

$$- \frac{yU''(y)}{U'(y)}\int_{x-U_\infty t}^{x} \frac{v(\xi,t) - v(\xi_1,t)}{\xi - \xi_1} d\xi_1 \tag{3.8}$$

For large times, v(x-U(y)t), l(x-t), and $\phi_0(x-t)$ tend to zero since they all tend

to zero when $|x|$ goes to ∞. Moreover, we also know that for large times, ξ - ξ_1 tends to a finite value (see equation (3.3)). Consequently, v(x fixed,t) of the form $\frac{f(x only)}{t}$ is solution of the above equation for large times, and v decays as $\frac{1}{t}$ or faster for large times.

Equation (3.8) is of great concern in the case of a Couette flow. Linear stability theory, and especially Fjortoft criterion predicts than such a flow is stable since U' is non-zero for any y. This is consistent with the explicit expression of v:

$$v = -\frac{y}{U'(y)}\frac{[\varphi_0(x) - \varphi_0(x-t)]}{t} \tag{3.9}$$

This last equation will allow us to perform a comparison between our numerical model and this analytical solution.

3.3 Unstable case

3.3.1 Liftup equation for large U"

For the unstable case v is expected to grow exponentially with time. The U"-dependent term is supposed to dominate. The problem is that if this term is very large so that G_0 can be neglected, the liftup equation is non-solvable. This may occur, for instance, with a profile having a strong U" for a given y. Indeed for large times, ξ goes to -∞ and $l(\xi)$ goes to 0. The liftup can be written:

$$l = \frac{yU''(y)}{U'(y)}\int_{-\infty}^{x}\frac{l(\xi_1)}{\xi - \xi_1}d\xi_1 \tag{3.10}$$

This integral equation can be identified as a Volterra equation of the first kind. The integral over ξ_1 has to be considered as a Cauchy's principal value one. Therefore the kernel of the integral equation is bounded. Besides, numerically the lower limit of the integral is finite. This is sufficient to affirm that this equation has no solution [8]. This feature makes the implementation of numerical model tough since it has to degenerate well whenever the U"-dependent term becomes large.

3.3.2 Comparison with the linear stability theory

In view of checking the accuracy of our numerical model, and in order to appraise how it degenerates for the unstable case, the linear stability analysis will be our yardstick. For an infinitesimal two-dimensional wavelike disturbance v is of the form:

$$v(x,y,t) = V(y)exp[i\alpha(x - c_r t]exp(c_i t)$$

where V(y) is the amplitude of v, α, real, is the spatial streamwise wavenumber, $c = c_r + ic_i$ the complex speed of the wave. For inflectional profiles, the growth rate αc_i is positive so that it produces an exponential growth.

For this kind of disturbance, one can solve the Rayleigh equation, leading to the well-known eigenvalue problem. Namely, solving:

$$V''(y) - \left(\frac{U''}{U-c} + \alpha^2\right) V(y) = 0 \tag{3.11}$$

for particular values of α, and corresponding discrete values of c_r and c_i.

We expect the most unstable mode of our initial infinitesimal disturbance to appear in our numerical model for large times, in order to perform a direct comparison with the linear analysis.

Next chapter describes in depth the numerical model.

Chapter 4

Numerical model

In order to get the tree components of the fluctuating velocity, and the pressure, one has to solve numerically the liftup equation (3.2) or (3.4). Indeed, provided l(x,y,z,t) one can derive the other remaining unknowns.

4.1 Numerical scheme

4.1.1 Discretization

The chosen scheme for solving equation (3.4) is a first order accurate explicit time-stepping method. The semi-discrete equation is: for $t^n = n\Delta t = t$, (n integer iteration number, Δt: timestep)

$$l^n(x,y,z) = -\frac{y}{U'(y)} \int_{x-U_\infty t^n}^{x} \frac{\varphi(\xi^n,y,z,t^n) - \varphi(\xi_1,y,z,t^n)}{\xi - \xi_1} d\xi_1$$

$$- \frac{yU''(y)}{U'(y)} \int_{x-U_\infty t^n}^{x} \frac{l^{n-1}(\xi^n,y,z) - l^{n-1}(\xi_1,y,z)}{\xi - \xi_1} d\xi_1 \qquad (4.1)$$

where

$$l^n(x,y,z) = l(x,y,z,t^n)$$

$$\xi^n = x - U(y)t^n$$

and therefore the modified equation is:

$$l(x,y,z,t) - l^n(x,y,z) = \Delta t \frac{yU''(y)}{U'(y)} \int_{x-U(y)t}^{x} \frac{g(\xi,y,z,t) - g(\xi_1,y,z,t)}{\xi - \xi_1} d\xi_1 \qquad (4.2)$$

where g = $\frac{\partial l}{\partial t}$.

If we don't use the parametric y-independence assumption, equation (4.1) and (4.2) are slightly different but the treatment is essentially the same:

$$l^n(x,y,z) = \int_{x-U_\infty t^n}^{x} \frac{C(y,y_1)}{U'(y_1)} \frac{\varphi(\xi^n,y_1,z,t^n) - \varphi(\xi_1,y_1,z,t^n)}{\xi - \xi_1} d\xi_1$$

$$+ \int_{x-U_\infty t^n}^{x} \frac{C(y,y_1)U''(y_1)}{U'(y_1)} \frac{l^{n-1}(\xi^n,y_1,z) - l^{n-1}(\xi_1,y_1,z)}{\xi - \xi_1} d\xi_1 \qquad (4.3)$$

$$l(x,y,z,t) - l^n(x,y,z) = -\Delta t \int_{x-U(y)t}^{x} \frac{C(y,y_1)U''(y_1)}{U'(y_1)} \frac{g(\xi,y,z,t) - g(\xi_1,y_1,z,t)}{\xi - \xi_1} d\xi_1 \qquad (4.4)$$

Two different approaches may be used to solve (4.1). One can either treat this equation in the physical plane and build up the appropriate moving grid, or consider the quantity ξ constant, solve in a Lagrangian frame of reference and get back eventually to the physical plane. Let us explain the former approach more in depth. In the following the notation l(x,y,z,t) will be replaced by l(x,t) since y and z will appear as parameters.

4.1.2 Grid

Equation (4.1) contains a noticeable difficulty. In order to get $l(x,t)$, $l(\xi_1, t - \Delta t)$ with $x - t \leq \xi_1 \leq x$ is required. This implies that the grid on which the computation is performed has to shrink of $i\Delta t$ between iteration i and i+1 (See Figure 4.1).

The grid points may not coincide from one iteration to the next. In fact, the program uses a constant Δx on each grid. So, each timestep, the discrete values of l(x) are interpolated through a cubic-spline fit routine. All the integrals appearing in equation (4.1) are computed via a Gauss-Legendre polynomial integration routine.

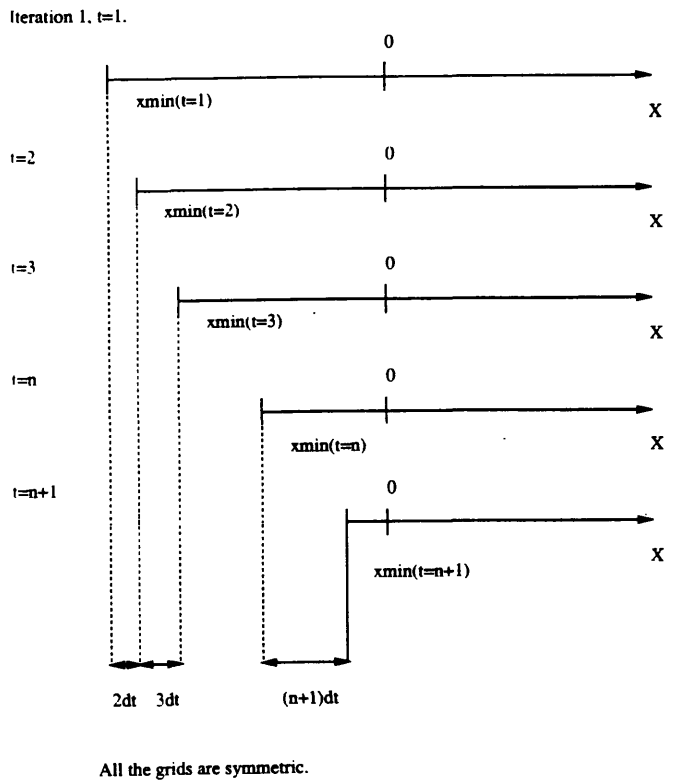

Figure 4-1: Computation Grid

4.2 Inputs

The two "physical" inputs in the program are:

- the initial disturbance which can be symmetrical or asymmetrical.
- the velocity profile U(y) which can be stable or unstable.

4.2.1 U profiles

An easy way to discriminate stable from unstable profiles, and to test the program with well-known ones (such as Blasius's and a separation profile), is to use Karman-Polhausen profiles. This family of polynomial profiles is defined as follows:

$$U_\Lambda(y) = 2y - 2y^3 + y^4 + \frac{\Lambda}{6}(y - 3y^2 + 3y^3 - y^4)$$

where $-12 \leq \Lambda \leq 12$ is a parameter, and $0 \leq y \leq 1$. These fourth order polynoms satisfy the conditions:

- U(y=0) = 0
- U(y=1) = 1 = U_∞
- U has a local maximum for y=0 and y=1.

For the peculiar values of Λ, 1 and -12, one recovers respectively the Blasius and separation flow profiles (See Appendix C). It is important to note that this family of profiles produces only reasonable U". Indeed, U" maximum is reached for Λ = -12 and is of order 10 for y=0.1. This might not be large enough to make the U"-dependent term dominate for an unstable profile. Besides, since y appears only as a parameter in the whole problem, one may input an artificially high U"(y) without worrying about the velocity profile. Conversely, without using the y-independence assumption, this family of profiles gives a strong singularity for y=1. Indeed, U'(y=1)=0, and this might cause the liftup to be too large for y=1.

4.2.2 Initial disturbance

In essence we will only use two particular disturbances.

- A symmetrical Gaussian-hat-like disturbance:

$$v_0(x,y,z) = -C(z)\frac{1}{L_x}exp(-\frac{x^2}{L_x^2})y^3exp(-\frac{y^2}{L_y^2}) \tag{4.5}$$

or

$$v_0(x,y,z) = -C(z)F(x)G(y)$$

where C(z) can be taken equal to unity without losing generality. The corresponding ϕ_0 satisfies:

$$\bar{\phi}_0(y,z) = \sqrt{\pi}C(z)G''(y) \neq 0$$

- A asymmetrical disturbance:

$$v_0(x,y,z) = -C(z)\frac{2x}{L_x^2}exp(-\frac{x^2}{L_x^2})y^3exp(-\frac{y^2}{L_y^2}) \tag{4.6}$$

whose corresponding $\bar{\phi}_0$ is 0. Of course, these initial disturbances respect the boundary conditions set up in Chapter 2: v vanishes for y=0, y=∞ and for large horizontal distances (See Appendix C).

L_x and L_y are typical streamwise and vertical length scales respectively. In practice, L_y will be taken equal to 1, since U(y) does not vary beyond y=1. The model is more particularly designed to predict the evolution of disturbances that are highly elongated in the streamwise direction. Thus L_x has to be large. Good results were obtained with L_x = size of the grid for the last iteration/20. This choice prevents the Gaussian hat to be too damped, and at the same time one can observe that the boundary conditions are fulfilled for fairly small x.

4.2.3 Timestep and spacestep

The other inputs are the spatial and temporal steps and y. The model has been built under the assumption that the velocities have a "boundary layer" character. So, y has to be small, of order one or less. The accuracy in x depends on the integration and curve-fit routines, but the program does not seem to be sensitive to the choice of Δx. However, as it will become apparent later, Δx has to be small enough to capture the oscillatory behavior of the U"-dependent term. Δx=10 represents a fair compromise between computation time and accuracy. As for the choice of the timestep, Δt must be small because the numerical scheme is only first order accurate. Practically good convergence is reached for Δt=1 or less. All these inputs allows us to get l(x,y,z,t). The next section describes the calculus of v(x,y,z,t), $\bar{l}(y,z,t)$ and $\bar{v}(y,z,t)$.

4.3 Outputs

The main output of the program is l(x,y,z,Tmax) $xmin$(last iteration) $\leq x \leq$ -$xmin$(last iteration).

The fluctuating velocity v is obviously given by taking the substantial derivative of l. Numerically, this is done using a central space backward Euler operator, using the same Δx and Δt than the main program.

The computation of the streamwise averages is a little bit trickier. Since, the grid shrinks and the waves propagate out of the computation domain, it is difficult to calculate these averages integrating from -∞ to ∞. Thus, we stop the integration as soon as the first derivative of l or v (for $\bar{l}$ and $\bar{v}$ respectively) is much less than one.

The next chapter describes the results obtained with the numerical model.

Chapter 5

Results

In this chapter, we are going to present the main results obtained with the numerical model defined in Chapter 4. A certain number of verifications are performed on the results in order to make sure that the code is right. An effective test consists in running the program with a Couette flow (e.g U"=0). This allows to verify the U"-independent term of the liftup equation (3.2): G_0.

5.1 Couette flow

The conspicuous interest of equation (3.4), using the parametric dependence in y, is that the exact analytical solution for v in the case of a Couette flow can be derived. Using equation (3.9) and the Gaussian-hat-like disturbance (4.5),

$$v(x,y,t) = \frac{y\sqrt{\pi}}{U'(y)} \frac{erf(\frac{x}{L_x}) - erf(\frac{x-t}{L_x})}{t} \tag{5.1}$$

where erf is the error function.

Figure (5.1) shows the comparisons between the v obtained numerically and the exact solution over time. The corresponding computed liftup is given as reference. The Cfl number is defined as usual:

$$Cfl = \frac{U(y)\Delta t}{\Delta x}$$

The results of the comparison with the analytical solution are satisfactory and validate the program as far as the computation of G_0. Slightly different results are obtained with the use of equation (3.2), where y appears as a variable and not a parameter. Especially, for the same symmetrical initial disturbance (See 4.3), the liftup goes to a finite value for large x, which is not zero. This discrepancy between the two boundary conditions can be easily understood if one considers the expression of G_0. For large time the liftup can be written:

$$G_0 = l(y) = \int_{x-U_\infty t}^{x} \frac{C(y,y_1)}{U'(y_1)} \frac{g(y) - g(y_1)}{\xi - \xi_1}$$

where g is only a function of y, since $\xi \to \infty$ and $\varphi_0(x,y,z) \to \varphi_0(y)$.

Then, if one gets rid of the y-dependence l(x large,y,z,t fixed) = 0. This explains the step function shape of the liftup when the dependence on y is included (See Figure 5.2). Figures (5.2) and (5.3) exhibits the evolution of the liftup and velocity over time, and give an insight of the global behavior of l and v for a Couette flow. The liftup and the vertical component of the velocity v propagate in the direction of positive x. The liftup tends to a finite value for large x and the amplitude of v decreases over time as expected. These features will be studied in depth in the following section.

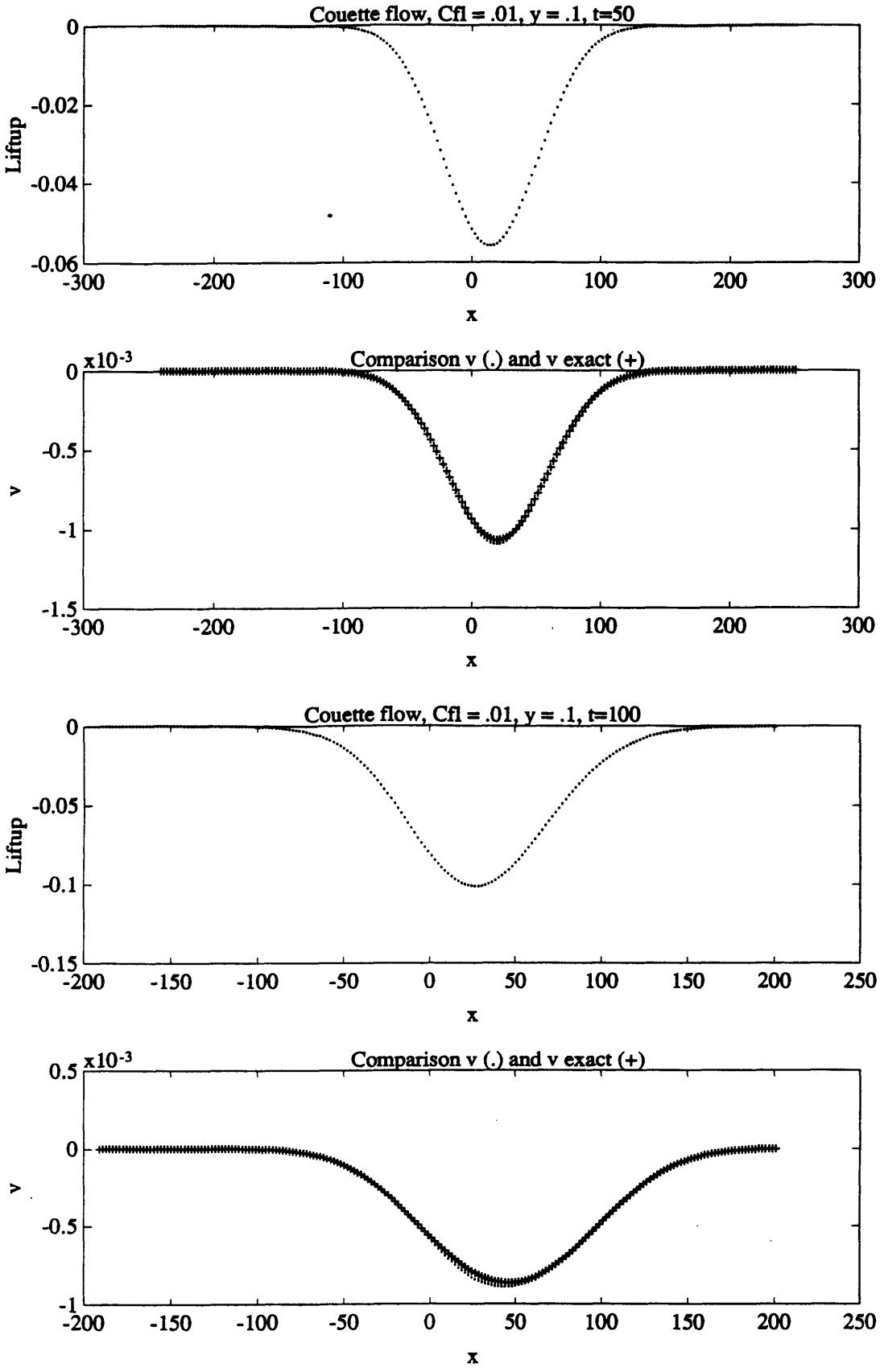

Figure 5-1: Liftup and comparison between $v_{computed}$ (.) and v_{exact} (+) for t=50 and 100. Δx =10, Δt =1, y=0.1

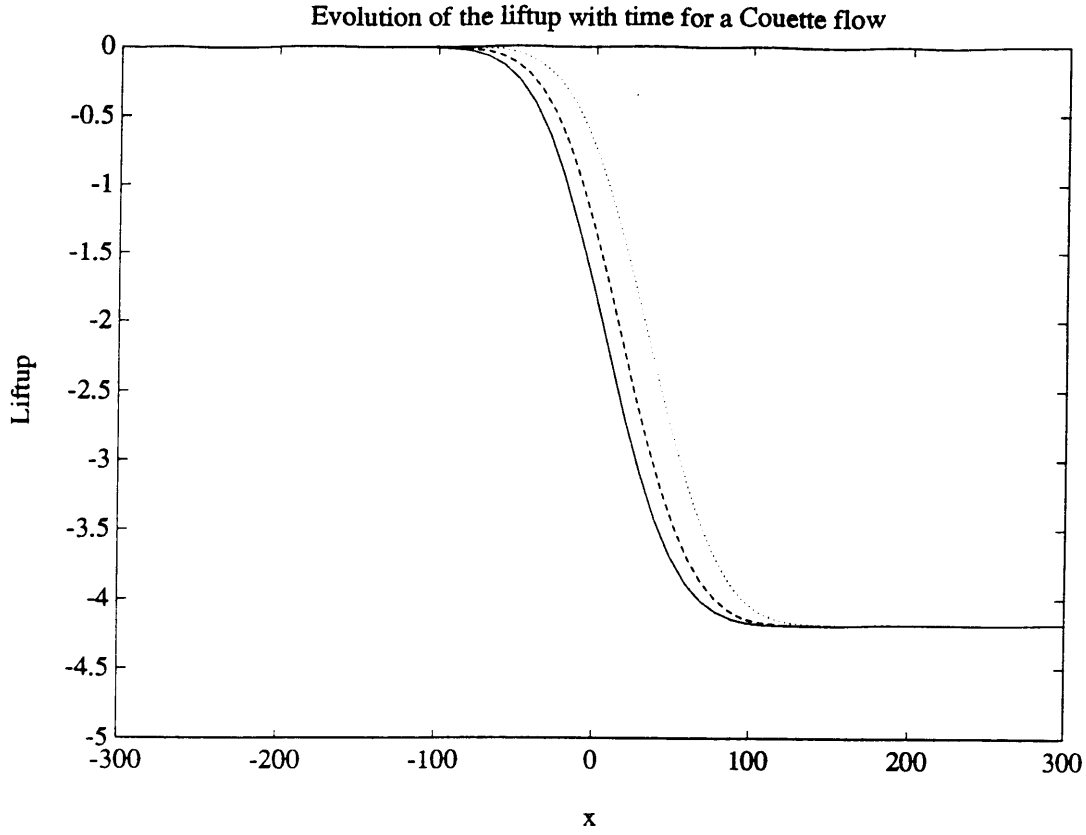

Figure 5-2: Evolution of the liftup over time, t=20 (continuous), 50 (-), 100 (.). Δx =50, Δy =0.1, Δt =1, y=0.5

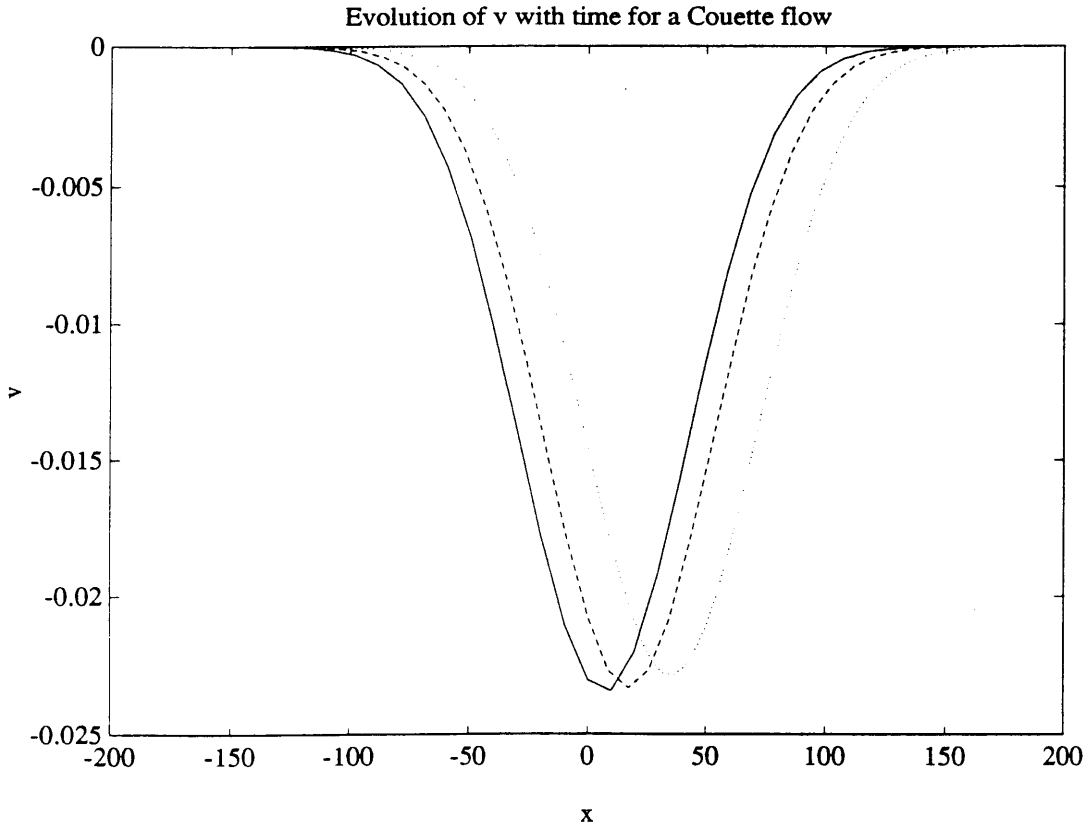

Figure 5-3: Evolution of v over time, t=20 (continuous), 50 (-), 100 (.). Δx =50, Δy =0.1, Δt =1, y=0.5

5.2 Stable profiles

All the results presented in the following sections are obtained with the code using a parametric dependence on y. The two initial disturbances used are the symmetrical and asymmetrical ones described in chapter 4. Lambda is chosen equal to the unity, corresponding to a Blasius-type profile. The study of stable profiles will be considered as a yardstick in view of pinpointing the phenomenon that underlies the behavior of unstable profiles. Thus we have to ascertain that our numerical results are accurate and in good agreement with the theory.

5.2.1 Liftup

Figure (5.4) represents the evolution of the liftup with time for the symmetrical initial disturbance. Several features have to be pointed out. First, the boundary conditions for $|x| = \infty$ are very well satisfied. For very large times, the liftup should tend towards a finite value. This does not appear clearly on Figure (5.4), since the last computation corresponds to t=200 only. Such a calculus was time-consuming and was not pursued any further. In any case, Figure (5.6) shows that v decreases and will tend to zero for large times which proves that the liftup complies with this requirement (e.g $\lim_{t\to\infty} l = l_\infty = cst$). The liftup does not propagate very fast because y is picked up near the wall, y=0.1, and consequently, the mean flow velocity is small: U(y)=0.2. It is hard to define a phase velocity for this disturbance, but one can notice that the first peak of the liftup moves at a larger speed than U.

The liftup's amplitude grows with time while its streamwise span increases. According to equation (3.7), the streamwise dimension of the perturbed region has to increase linearly with time. Conversely, for the asymmetrical initial disturbance, $\bar{l}_0$=0 implies that $\bar{l}$=0 at any time. Figure (5.5) shows the evolution of $\bar{l}$ for these two disturbances. The linear growth $\bar{l}$ is very well obtained. The slope of the straight line, which is nothing but $\bar{v}_0$, corresponds exactly to the computed $\bar{v}_0$. This proves that the program gives consistent (See Figure 5.7).

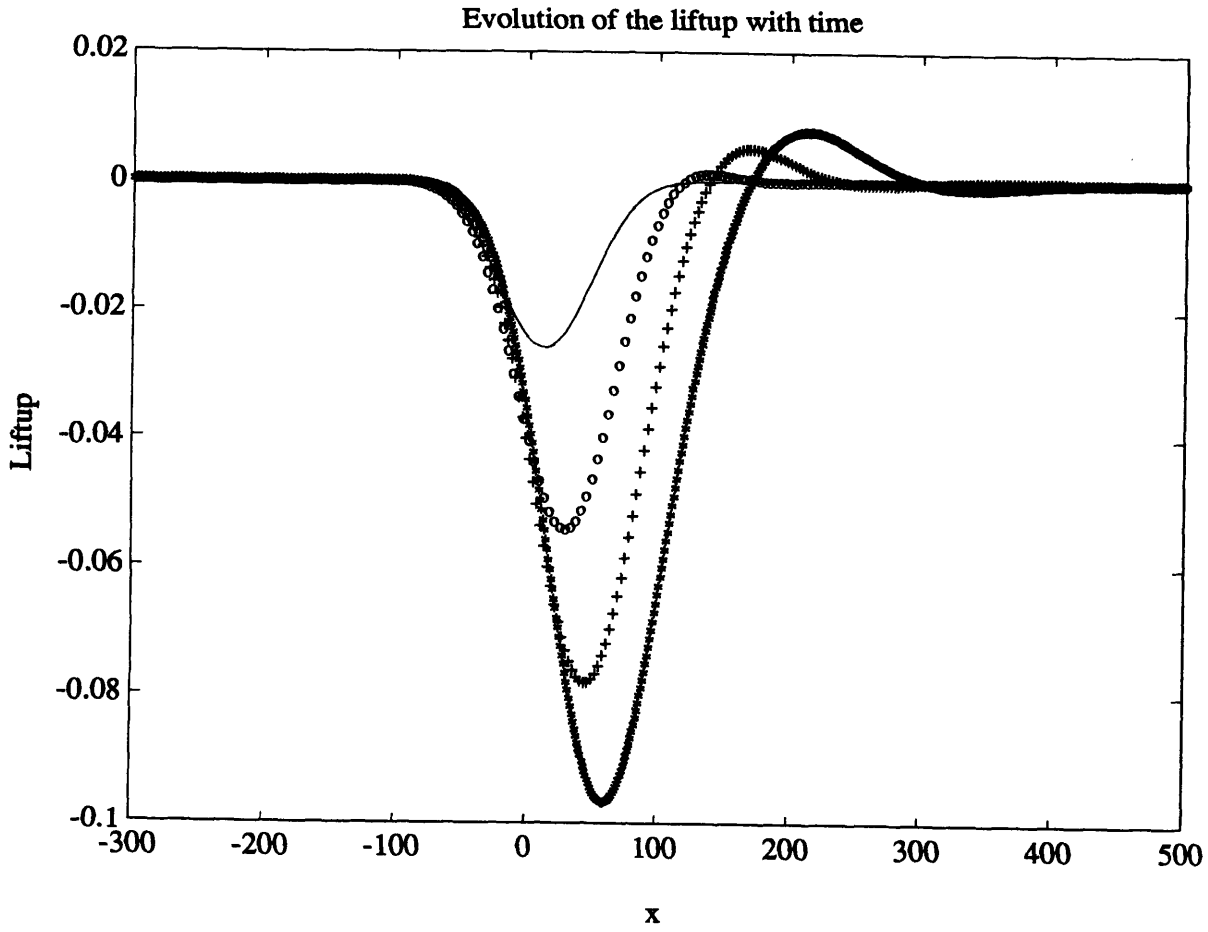

Figure 5-4: Evolution of l over time, t=50 (continuous), 100 (o), 150 (+), 200 (*). Δx =10, Δt =1, y=0.1, Λ =1

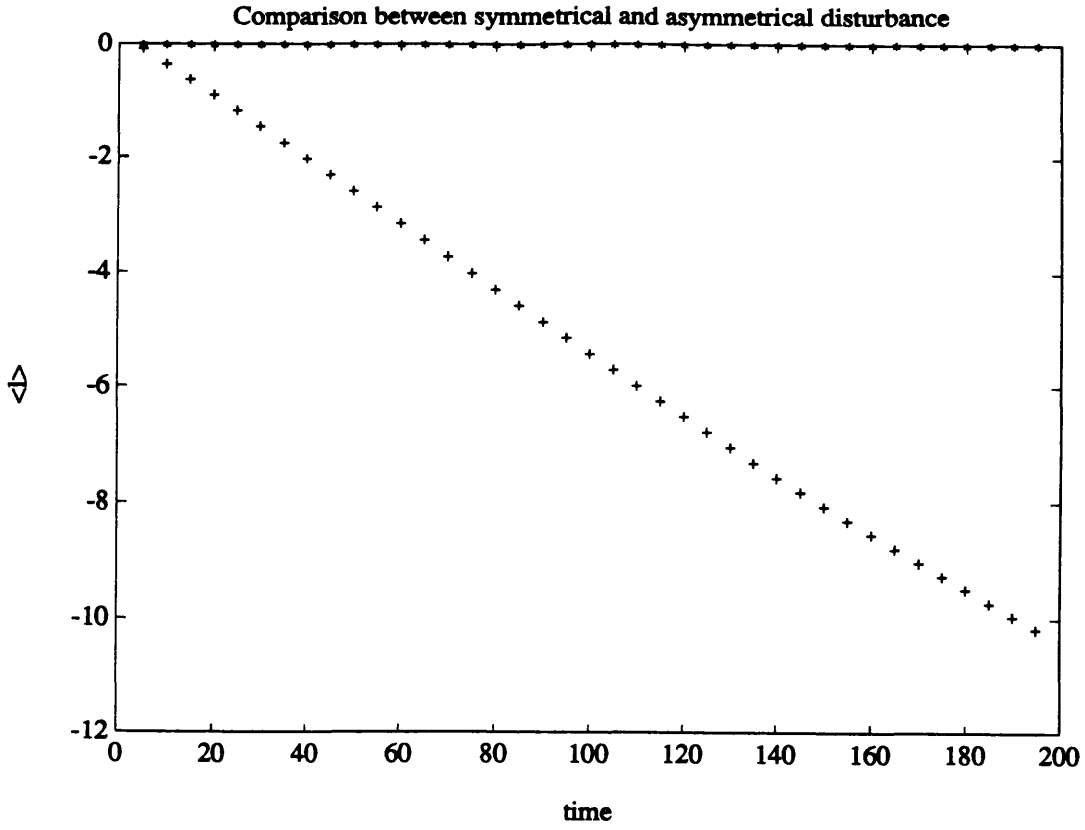

Figure 5-5: Evolution of $\bar{l}$ for the symmetrical (+) and asymmetrical (*) disturbances. Δx =10, Δt =1, y=0.1, Λ =1

5.2.2 Vertical component of the fluctuating velocity v

Figure (5.6) exhibits the corresponding velocities v to the set of liftups showed on Figure (5.4). Here again, the boundary condition $\lim_{|x|\to\infty} v = 0$ is pretty well met. The amplitude of v decreases, but since $\bar{v}$ has to remain constant, v possesses a "growing wiggle" that allows $\bar{v}$ to match the value of $\bar{v}_0$. The computed value $\bar{v}$ is constant over time, and equals zero for an asymmetrical disturbance as shown on Figure (5.7). For x fixed, v decays (See Figure (5.8)). For t larger than 300, v decreases as $\frac{1}{t}$ as expected (See Figure (5.9)). In fact v is of the form:

$$v = \frac{\alpha}{t} + \epsilon$$

where $\epsilon \leq 0.001$.

A final remark may be underlined as far as the difference of behavior of symmetrical and asymmetrical disturbances. The algebraic instability theory predicts the appearance of an instability for a flow that has a non-zero initial vertical momentum (e.g $\bar{\phi}_0 \neq 0$). Indeed we observed a streamwise spreading of our symmetrical disturbance. This feature is also present for our asymmetrical disturbance, the main difference lying in the fact that the liftup amplitude has to decrease in order to abide by the rule $\bar{l}$=0. (See Figure 5.10)

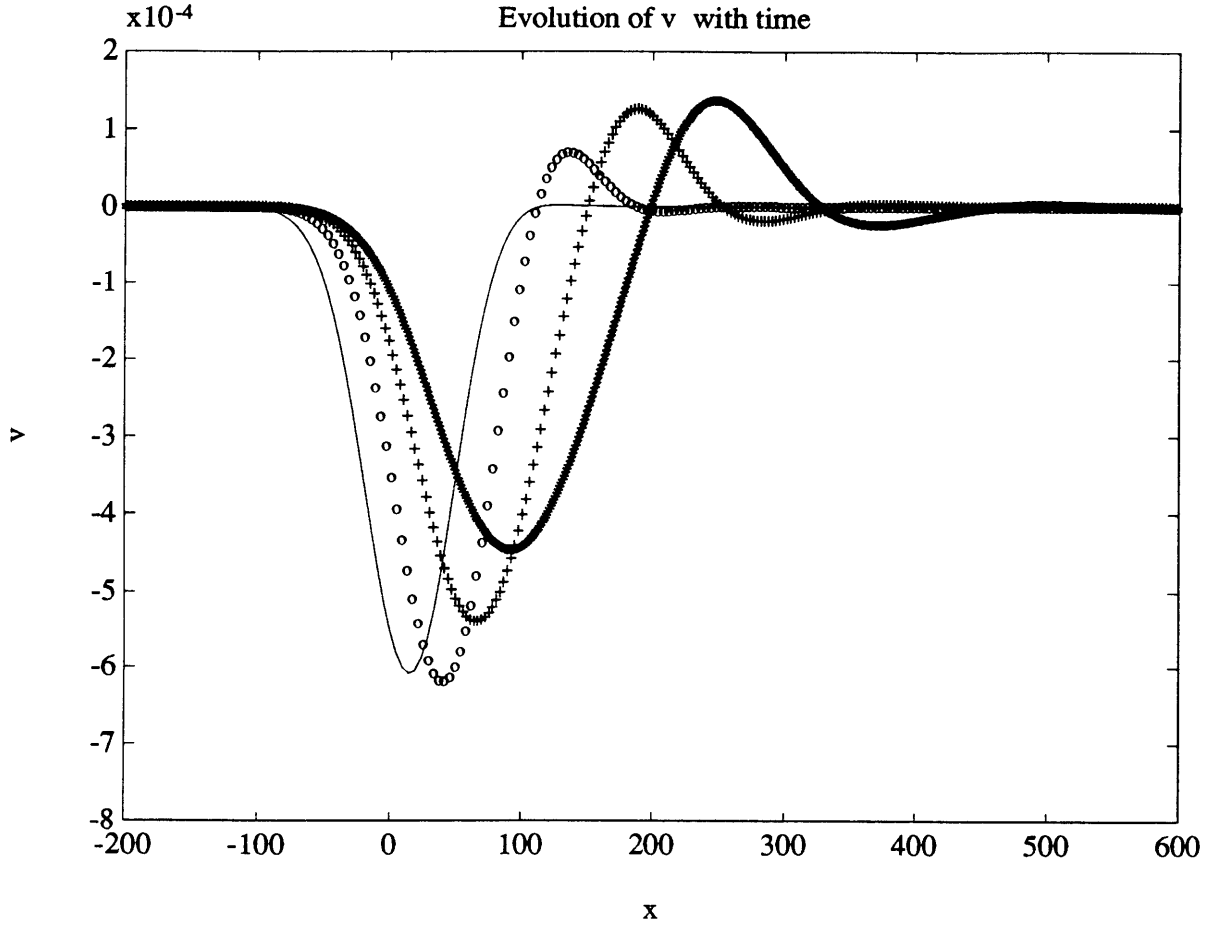

Figure 5-6: Evolution of v over time, t=50 (continuous), 100 (o), 150 (+), 200 (*). Δx =10, Δt =1, y=0.1, Λ =1

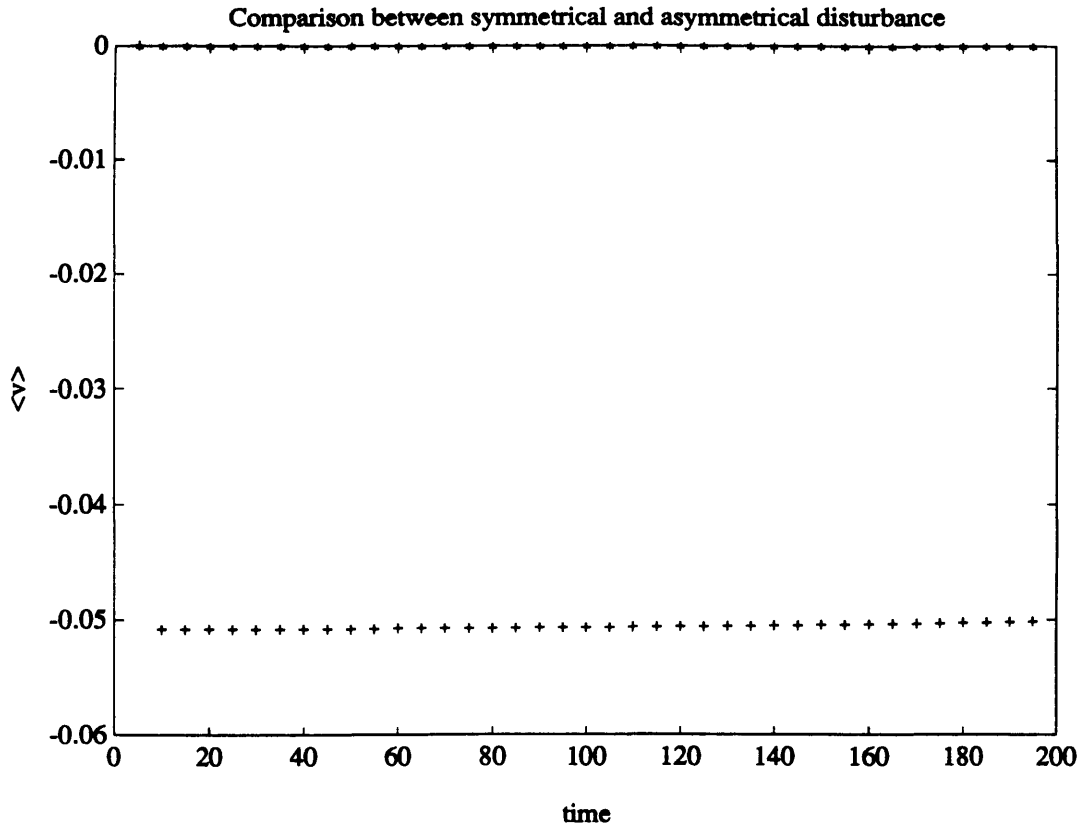

Figure 5-7: Evolution of $\bar{v}$ for the symmetrical (+) and asymmetrical (*) disturbances. Δx =10, Δt =1, y=0.1, Λ =1

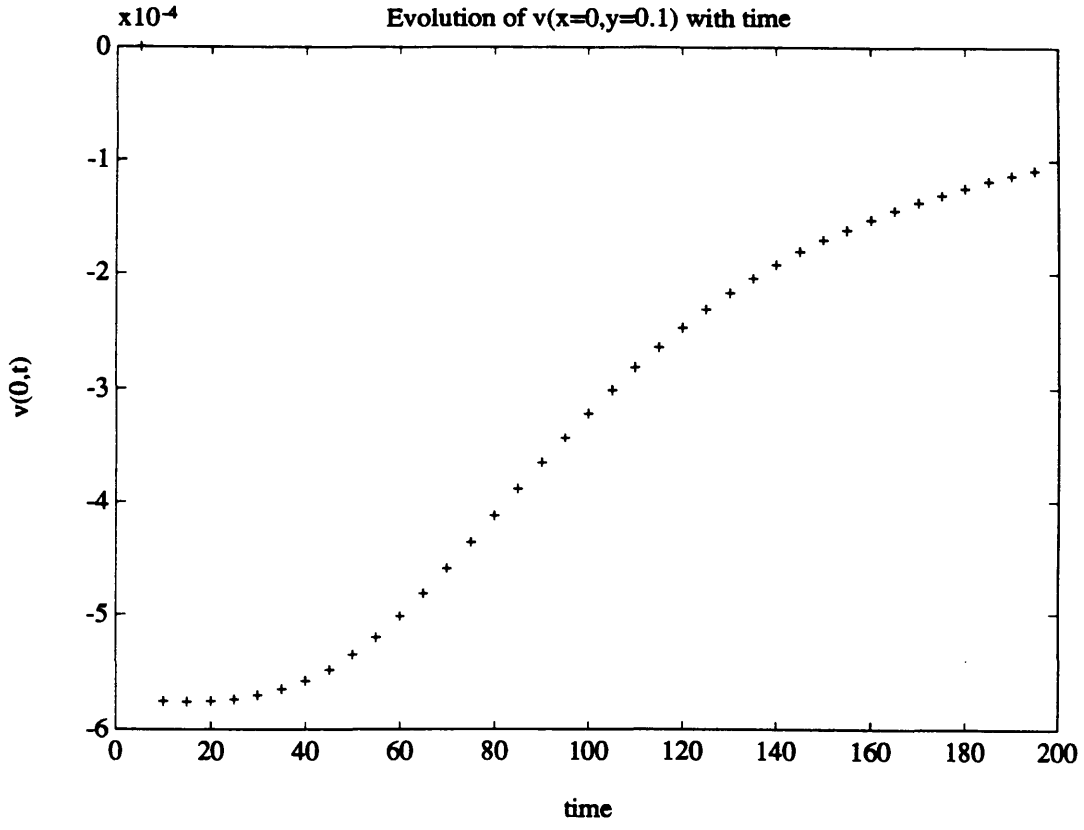

Figure 5-8: Evolution of v(x=0, y=0.1) with time. Δt = 1, Λ =1

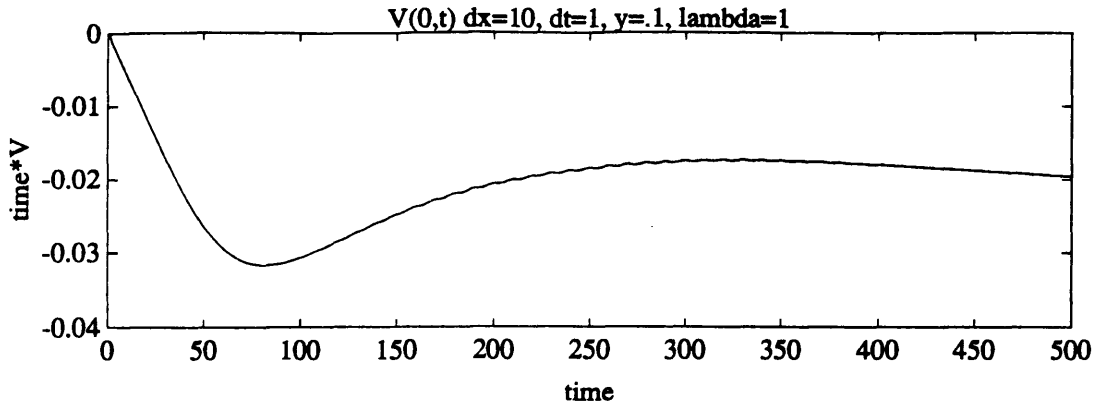

Figure 5-9: v(x=0, y=0.1)t vs time. Δt =1, y=0.1, Λ =1

The results agree, overall, very well with the theoretical work derived in chapter 3. Even if the numerical scheme is only first order accurate in time, it allows to display the principle characteristics of l and v for stable profiles. Computations performed with a smaller timestep than Δt =1, such as Δt =0.5 do not produce any significant difference which insures than Δt =1 provides a sufficiently good accuracy.

5.3 Unstable profiles

Obviously, the origin of the unstable behavior is contained in the U"-dependent term in equation (3.2) (that we will also term: "second term"). Thus it is certainly important to monitor the evolution of this term over time.

5.3.1 Study of the U"-dependent term

To begin with, the program was run with the symmetrical initial disturbance and the Von-Karman profile corresponding to Λ=-10. This value of lambda already gives a

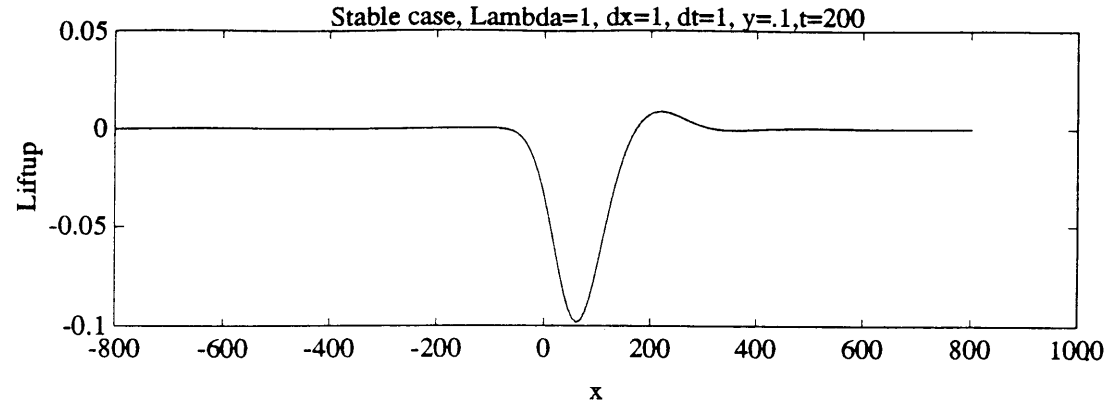

(a)

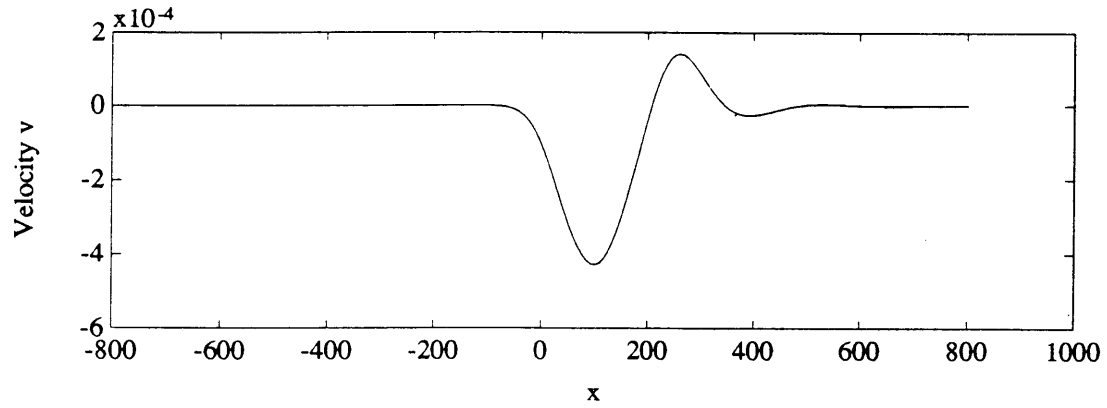

(b)

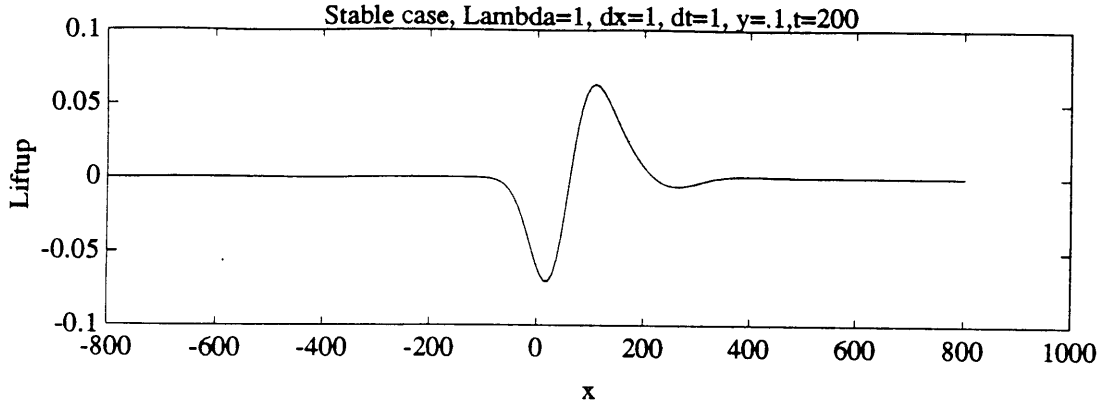

(c)

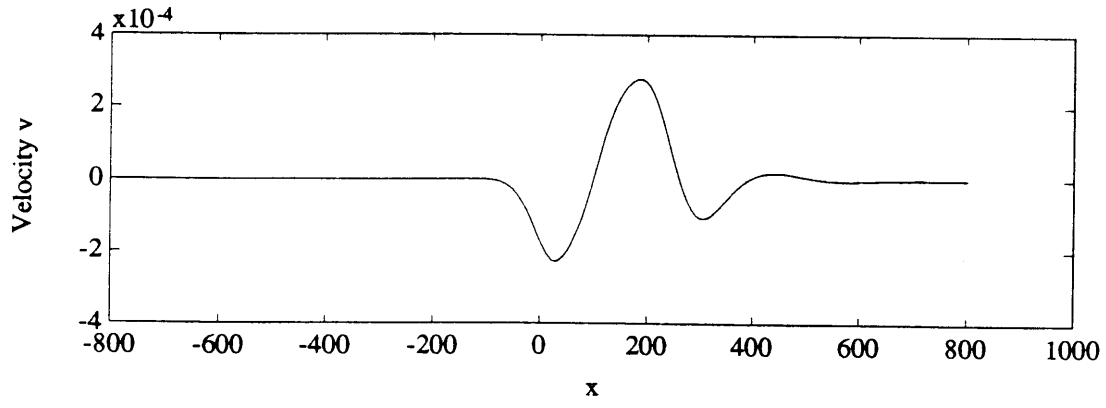

(d)

Figure 5-10: Difference of evolution of the liftup and v with x for a symmetrical ((a) and (b)) and an asymmetrical disturbance ((c) and (d)). Δx =10, Δt =1, y=0.1, Λ =1, t=200.

large U" without reaching the absolute instability that would be created by a reversal flow (Λ=-12). We did not find any growing instability as we were expecting. The shape of liftup is globally the same than in the stable case. However the contribution of the second term in (3.4) is bigger. Figure (5.11) show the contribution of the U"-dependent term for a stable and an unstable profile. Using these data, the ratio r of the amplitude of U"-dependent term over the amplitude of G_0 is:

- r = 0.035 for the stable case
- r = 0.166 for the unstable case

This may be explained by the larger value of U"(y) in the unstable case, for the value of we picked, and could also obtained for stable profiles. The particularity of unstable profiles is that the sign of the second term does not vary over time and is the same than the sign of G_0. Thus in the case of stable profiles, for large x, the contribution of the second term tends to decrease the liftup. The opposite effect holds for unstable profiles and might entail a growth for large times.

Figure (5.13) shows the growth rate of the amplitude of U"-dependent term, respectively. The growth rate of the U"-dependent term is larger for unstable profiles. For a stable, one can see that the growth rate of the second term is very slow.

These remarks lead to the conclusion that an instability should show up for very large time. But our program possesses an inherent limitation that must be emphasized. Since we chose to compute l on a moving grid, when t increases, for a constant Δx, we need more and more points. With a workstation such as a DEC 3100, we can hardly reach t=200, and this might not be enough. Indeed, such a growth was not detected using Von-Karman profiles, however the previous plots suggest that the key factor to foster growth is to have a strong positive U".

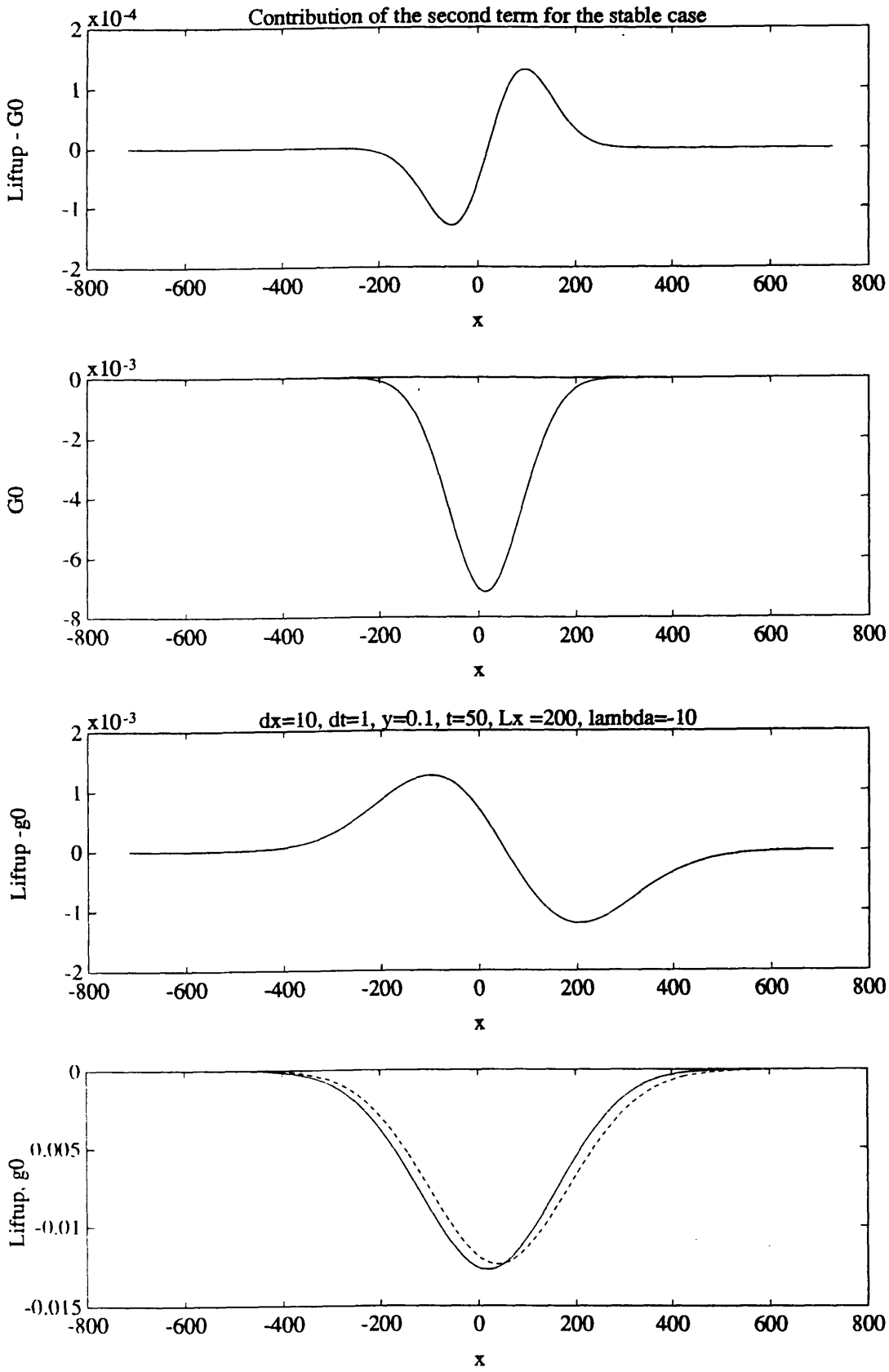

Figure 5-11: Contribution of the U"-dependent term to the liftup for the stable and the unstable case. Δx =10, Δt =1, y=0.1, Λ =1 and -10, t=50

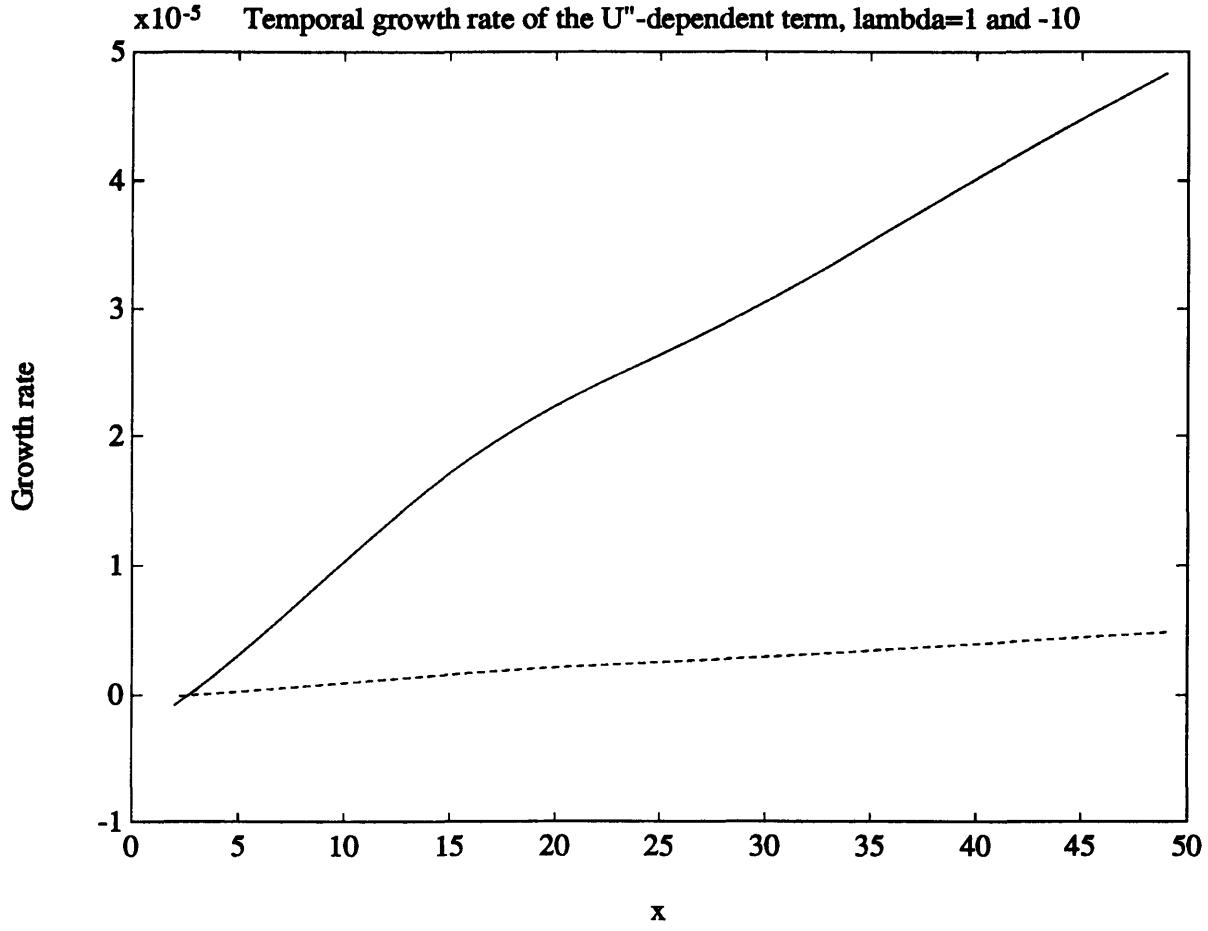

Figure 5-12: Temporal growth rate of the U"-dependent term. Δx =10, Δt =1, y=0.1, Λ =1 (-) and -10 (continuous), t=50

5.3.2 Evolution of the liftup for a large U"

One can input artificially a large U"(y) in the liftup equation (3.4), keeping the same value of U and U' for a given y. We input the following parameters: y=0.1, U = $U_{\Lambda=-10}(y)$, U'= $U'_{\Lambda=-10}(y)$, U"=95. This technique might not be legitimate since the parametric dependence on y cancels the impact of the whole mean flow profile. But the aim of this test is not to find the exact solution of (3.2) but rather to understand qualitatively what might trigger an exponential growth. The results of the run are shown on Figure (5.13) and (5.14), and the following features can be underlined:

- the U"-dependent term has a large temporal growth rate
- it propagates faster than G_0
- it stretches over larger streamwise distance with increasing time
- for t greater than a critical time t_c a wave-packet crops up

These results seem to suggest that a large positive U" spurs streamwise spreading of the liftup. This is due to the major contribution of the U"-dependent term, which propagates downstream faster than G_0 affecting the liftup on its way for large x-distances.

According to Figure (5.14) the U"-dependent term ends up having a wave-packet-like shape. The problem is that the computation depends on the timestep as soon as this wave-packet shows up (e.g $t \geq t_c$). This might be explained by the fact that for t greater than t_c the U"-dependent dominates and transforms the liftup equation in a non-solvable equation as already mentioned in Chapter 3. This might be avoided via a second order development of v and might allow the program to accommodate the evolution of this wave packet without timestep dependence. Unfortunately, this would make the liftup equation (3.2) a lot harder to solve.

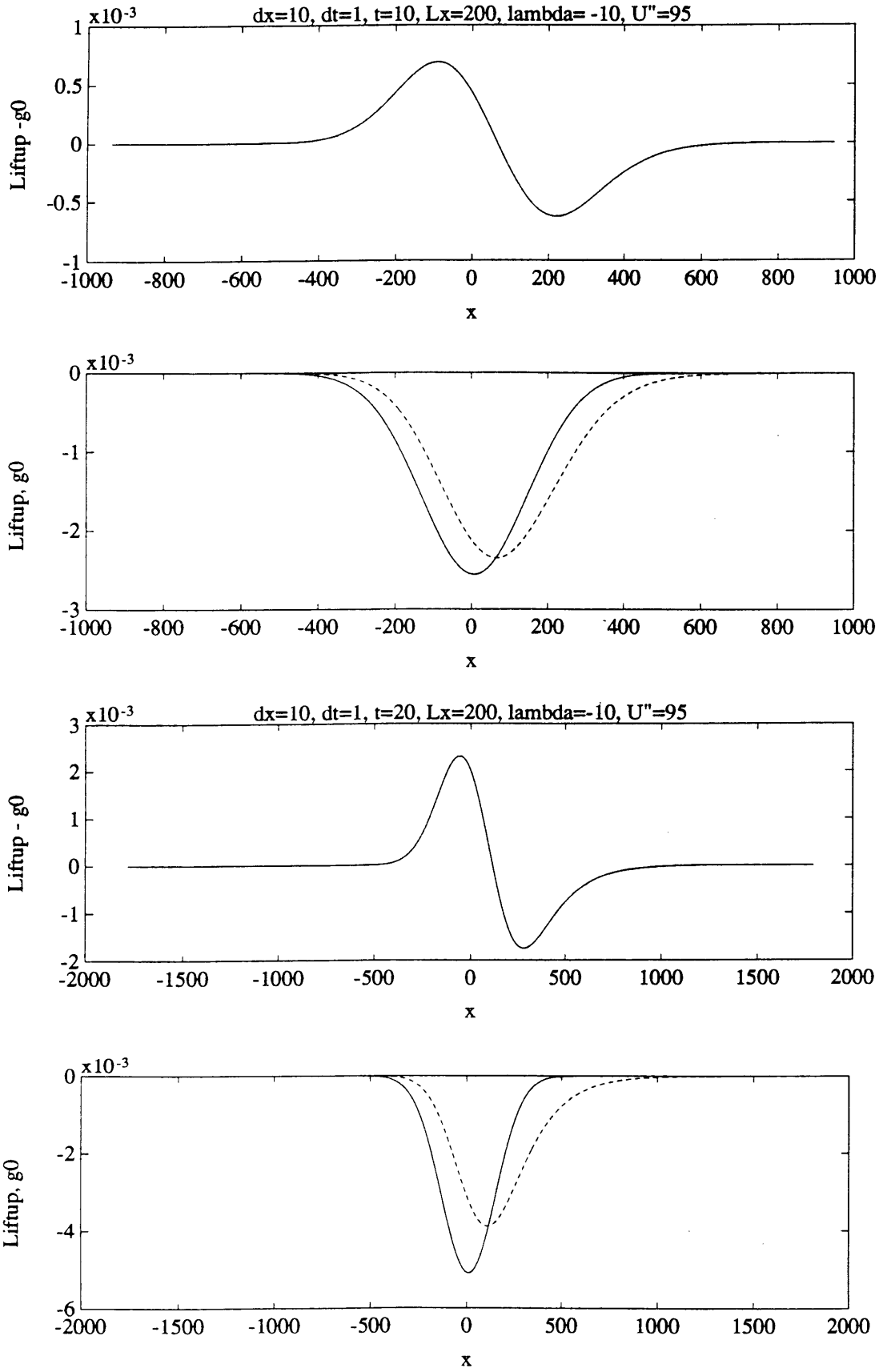

Figure 5-13: Contribution of the U"-dependent term to the liftup for a profile having a large U"at y=0.1. Δx =10, Δt =1, y=0.1, U"(0.1)=95, t=10 and 20. Figures (b) and (d): G_0 (continuous), liftup (-)

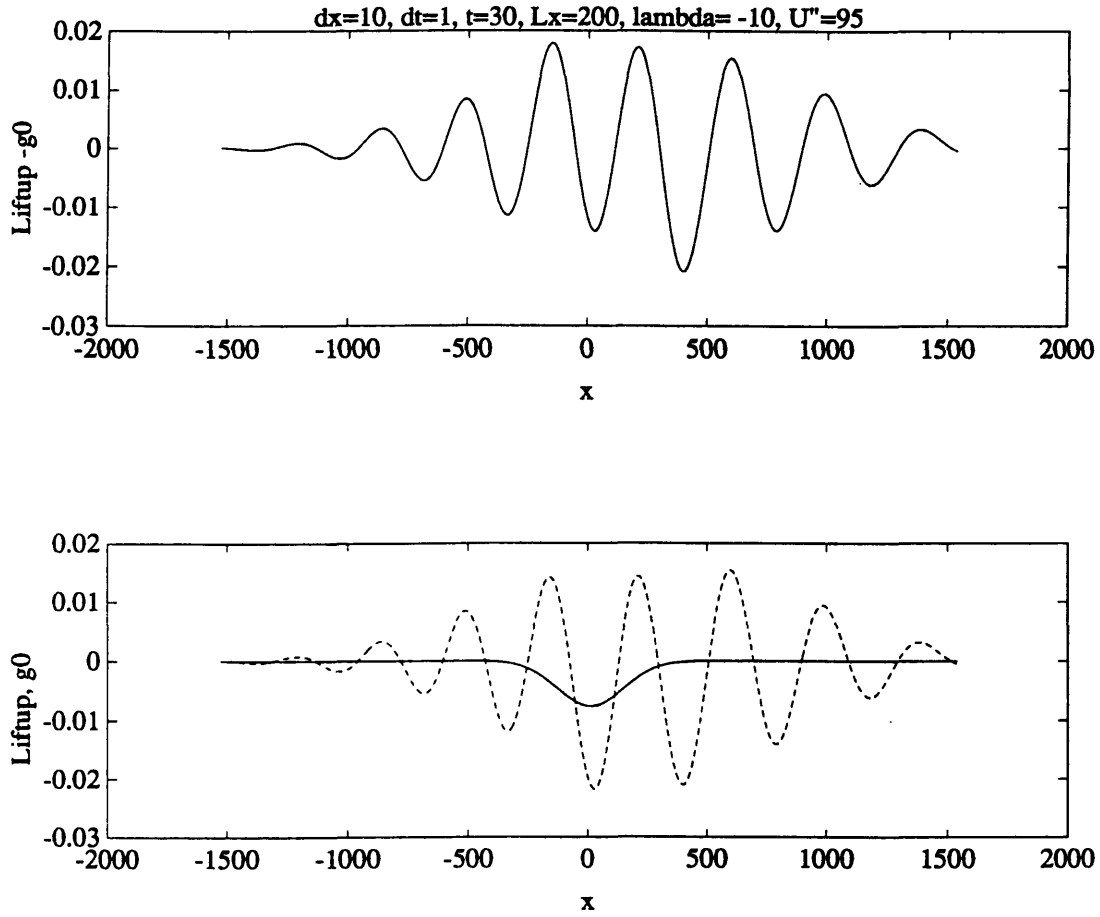

Figure 5-14: Contribution of the U"-dependent term to the liftup for a profile having a large U"at y=0.1. Δx =10, Δt =1, y=0.1, U"(0.1)=95, t=30. Bottom figure: G_0 (continuous), liftup (-)

Chapter 6

Conclusions

Despite the extreme idealizations on which the proposed model is based, it is able to point to plausible mechanisms for the evolution of a three-dimensional disturbance in a wall layer. Central to this model is Landahl's method that consists in breaking up the evolution of such a disturbance in three different and appropriate time scales. The first one, namely the early shear interaction stage, allowed an inviscid and linear treatment of the evolution. The solutions for the liftup of a fluid element and for its corresponding fluctuating vertical velocity component, using the so-called near wall approximation, show good agreement with the classical theory.

- For a stable mean velocity profile: the liftup propagates so that the streamwise average of the region it perturbs, grows linearly with time. This streamwise stretching might explain the formation of streamwise streaks as explained by the algebraic instability theory. The vertical component of the velocity v decreases as $\frac{1}{t}$ and has a constant streamwise average as expected.

- For an inflectional mean velocity profile: we did not find the exponential growth predicted by Rayleigh's theory. Nevertheless, the U"-dependent term of the liftup equation is larger and grows faster than in the case of a stable profile. The model suggests that a growth could be obtained for profiles having large U" below the inflection point. This hypothesis could not be ascertained because of numerical limitations on the one hand and the use of a first order approximation

for v on the other hand.

Further researches should concentrate on:

- finding an analytical solution for the liftup. This would eliminate the difficulty that one has to discriminate the real instability, for an inflectional profile, from a pure numerical instability. The starting point of this search could be the alternative equation for the liftup given in appendix B, considering the liftup as a function of ξ and t and not ξ alone. Another possibility would consist in deriving a new equation for the liftup, using the second order development of v and the slender body approximation that could go along with the involved third order integral.

- implementing a numerical scheme with a better accuracy. One could devise a second order accurate (in time) scheme. This would allow the use of fewer iterations to reach convergence which would lead to a better description of the long time behavior of the flow. Once again a second order approximation of v would be necessary.

- In each case, one should compare the wavelength of the obtained wave-packet with the linear theory, as suggested in Chapter 3.

Appendix A

Why the liftup cannot be a function of ξ alone

Starting with equation (3.4) (which includes the parametric dependence of y), one finds after an integration by part over ξ_1 and for $t \to \infty$:

$$l \equiv l_\infty(\xi) = \frac{y}{U'(y)} \int_{-\infty}^{\infty} [ln|\xi - \xi_1|[\phi_0(\xi_1) + U'' l_{\infty\xi}(\xi)]d\xi_1] \qquad \text{(A.1)}$$

where the subscript ξ denotes $\frac{\partial}{\partial \xi}$. One can get an explicit expression for the liftup by taking the Fourier transform of l with respect to ξ, using the "Faltung theorem".

Notations:

- ν is the transformed variable for ξ
- Upper cases denote transformed quantities: e.g L(ν) is the transform for l(ξ)
- sg is the sign function

The Fourier transform for "ln(ξ)" is obtained using generalized functions (See Lighthill [7]) and equals:

$$\frac{-sg(\nu)}{2\nu}$$

Thus equation A.1 gives:

$$L(\nu) = -\frac{y}{2U'(y)} \frac{\Phi_0 sg(\nu)}{\nu[1 + ia(y)sg(\nu)]} \tag{A.2}$$

where

$$a(y) = \frac{yU''(y)\pi}{U'(y)}$$

The liftup equation in the Fourier plane can be inverted back in:

$$l(\xi) = \frac{yU'(y)}{U'^2 + (yU''\pi)^2} \int_{-\infty}^{\infty} ln|\xi - \xi_1|\phi_0(\xi_1)d\xi_1$$

$$- \frac{yU'(y)U''(y)\pi}{U'^2 + (yU''\pi)^2} \int_{-\infty}^{\xi} \phi_0(\xi_1)d\xi_1 \tag{A.3}$$

This last equation was eventually relinquished since no singularity can occur for unstable profiles. U" is squared in all the denominators, which cancels the impact of U" on the flow stability.

Appendix B

An alternative equation for the liftup

As seen in appendix B, the liftup cannot be a function of ξ alone. The idea here, is to stress the time dependence by getting a first or partial differential equation in x and t for the liftup.

Using equations (2.16) and (2.21) we have:

$$\frac{Dl}{Dt}(x,y,z,t) = \int_0^\infty C(y,y_1)\phi_0(\xi_1,y_1,z)dy_1 + \int_0^\infty C(y,y_2)U''(y_2)\left(\frac{\partial l}{\partial x}\right)_{x,y_2,z,t} dy_2 \tag{B.1}$$

Reminder: ξ, ξ_1 and ξ_2 are respectively equal to x -U(y)t, x-U(y_1)t and x-U(y_2)t. The trick consists in plugging the expression of the liftup (3.1) in equation (B.1). Using the symmetry in ξ_1 and ξ_2 and the parametric dependence in y for large times, the new equation for the liftup is:

$$\frac{Dl}{Dt}(x,y,z,t\to\infty) = -y\int_0^\infty \phi_0(\xi_1,y_1,z)dy_1 - yU''(y)\int_0^\infty \left(\frac{\partial G_0}{\partial x}\right)_{x,y_1,z,t} dy_1$$

$$+\frac{2}{t}\left(\frac{yU''(y)}{U'(y)}\right)^2 \int_{x-U_\infty t}^{x}\int_{x-U_\infty t}^{x} \frac{l_x(\xi_1,y,z,t)}{\xi_1-\xi_2}d\xi_1 d\xi_2 \qquad \text{(B.2)}$$

Where G_0 is defined in equation (3.1) and the subscript x denotes $\frac{\partial}{\partial x}$.

This equation can be solved via an implicit numerical scheme. The appearance of the "$\frac{1}{t}$-term" implies that such a scheme is only stable for a large number of iteration. Therefore it is not easier to cope with this equation than the basic equation (3.2).

Appendix C

Mean flow profiles and initial disturbances

This appendix presents the profiles and initial disturbances used in the numerical model.

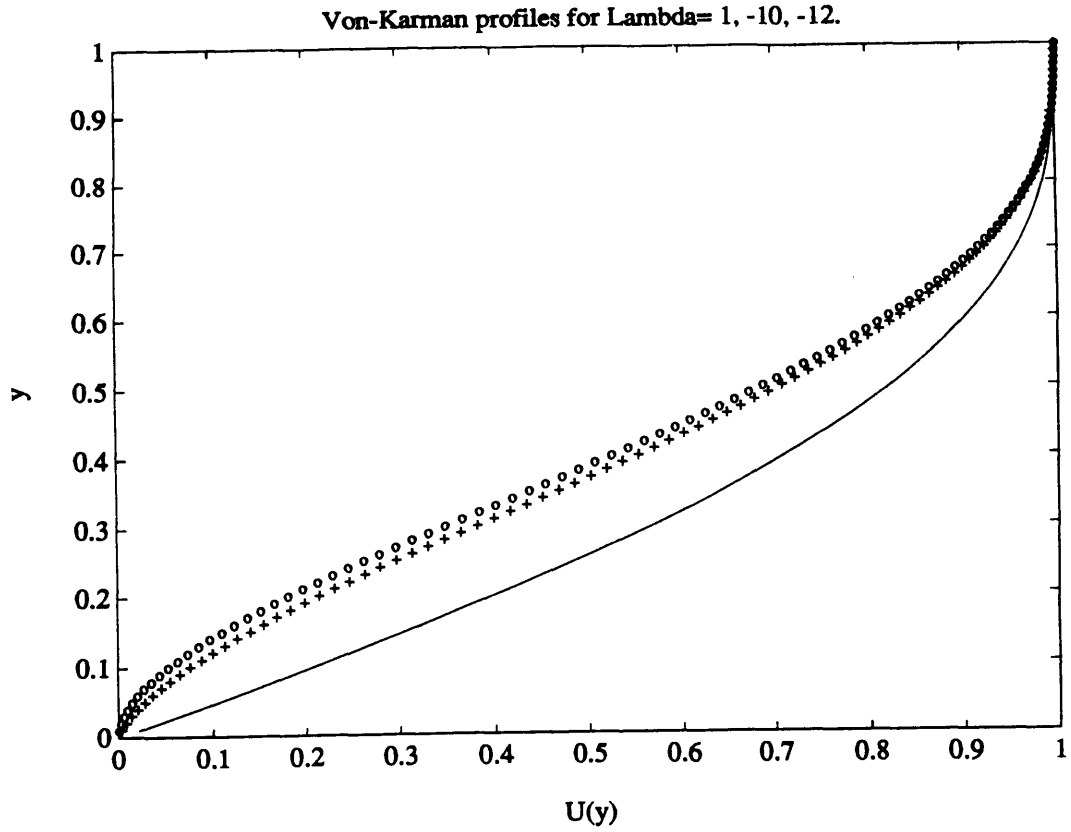

Figure C-1: Karman-Polhausen profiles: Stable Blasius profile Λ =1 (continuous), unstable profile (+) Λ =-10, separation profile (o) Λ =-12

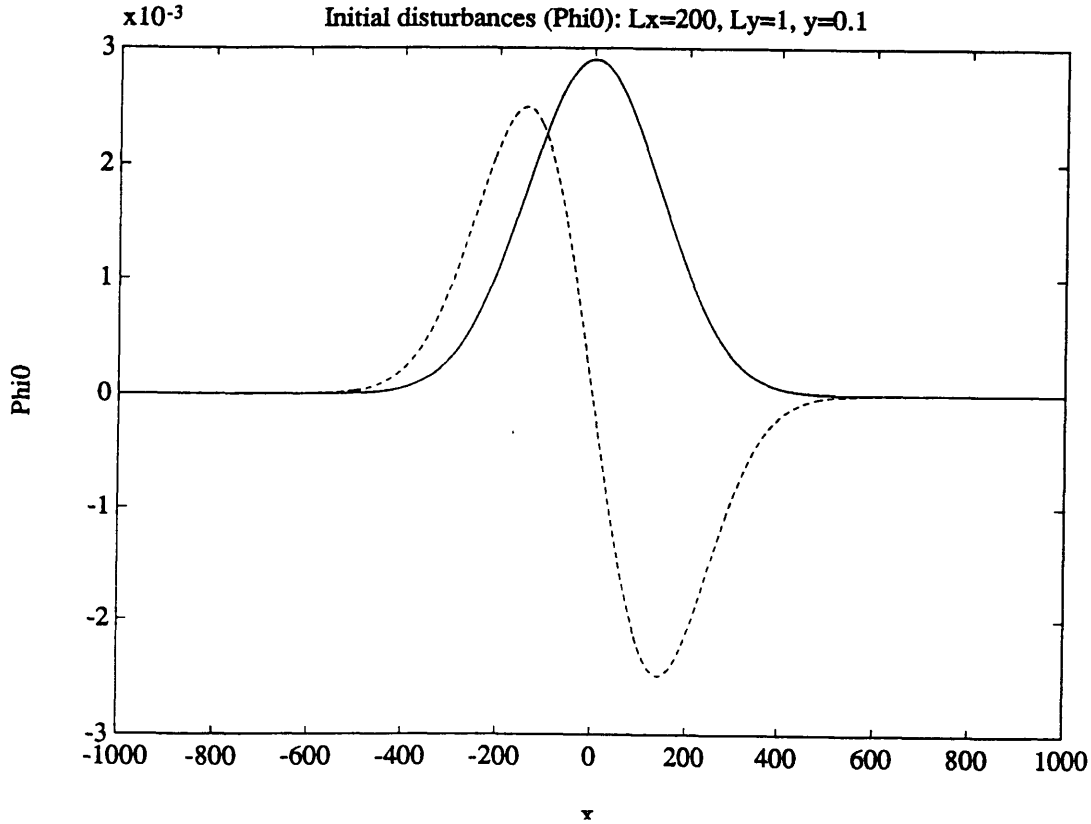

Figure C-2: ϕ_0 for a symmetrical (continuous) and an asymmetrical disturbance (-), L_x=200, L_y=1, y=0.1

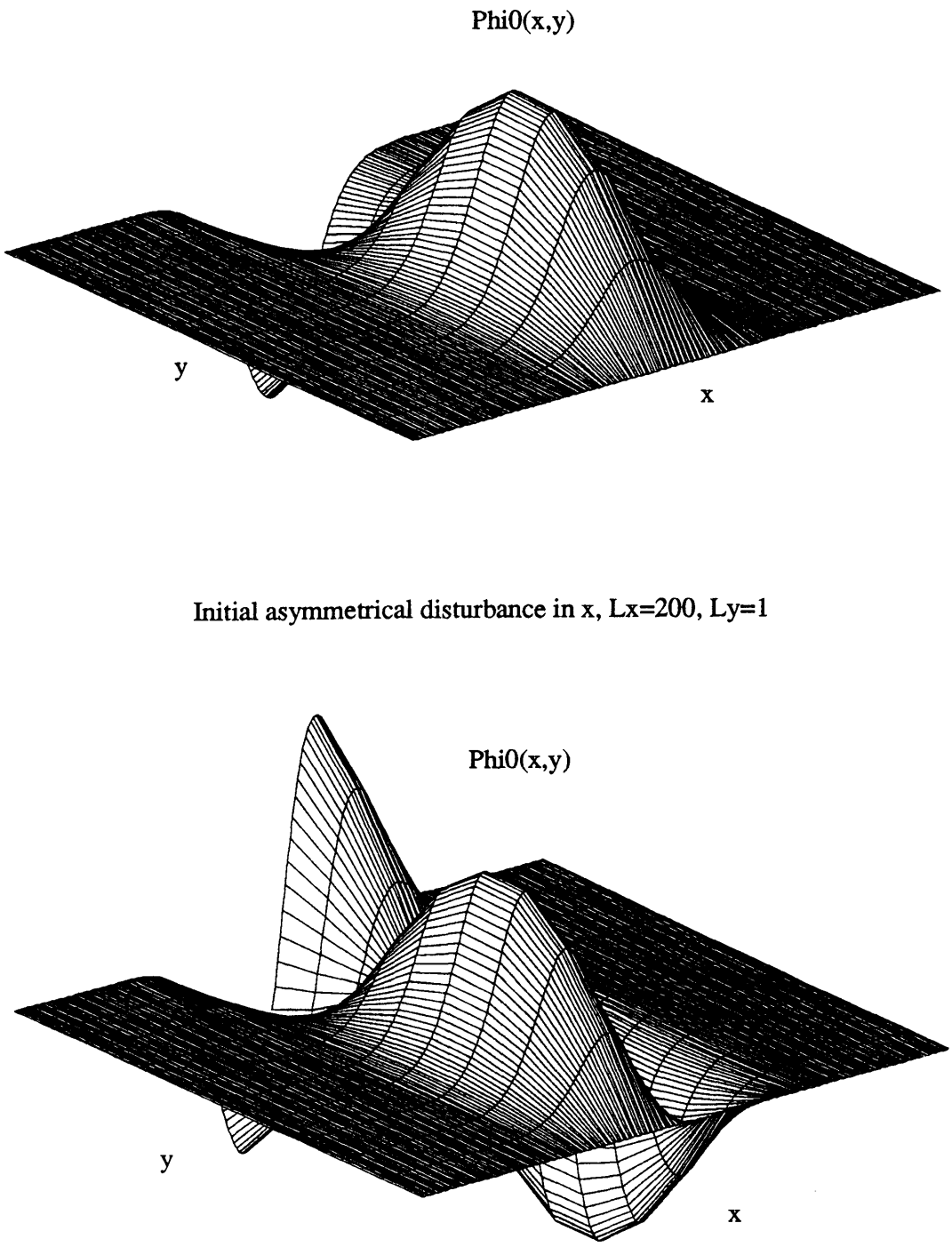

Figure C-3: Global shape of ϕ_0 for a symmetrical and an asymmetrical disturbance, L_x=200, L_y=1

Bibliography

[1] T. Ellingsen and E. Palm. *Phys. Fluid., 18-487*, 1975.

[2] M.T Landahl. A note on algebraic instability of inviscid parallel shear flow. *J. Fluid Mech., 98-243*, 1980.

[3] M.T Landahl. Boundary layer turbulence regarded as a driven linear system. *Physica North Holland, Amsterdam*, 1989.

[4] M.T Landahl. On sublayer streaks. *J. Fluid Mech, 212-243*, 1990.

[5] M.T Landahl. The role of algebraic instability in transition to turbulence. *unpublished*, 1992.

[6] M. Lesieur. *Turbulence in fluids.* Kluwer academic publishers, 1991.

[7] M. J. Lighthill. *Introduction to Fourier analysis and generalized functions.* Cambridge University Press, 1958.

[8] Morse and Feshback. *Method of theoretical physics.* Mc Graw Hill, 1953.

[9] W. M. F. Orr. *Proc. Roy. Irish Acad., A 17, 124*, 1907.

[10] L. Prandtl. Bericht uber untersuchungen zur ausgebildeten turbulenz. *Angew. Math. Mech., 5-136*, 1925.

[11] F.A Schraub S.J Kline, W.C. Reynolds and P.W Runstadler. The structure of turbulent boundary layers. *J. Fluid Mech., 50-133*, 1967.

[12] F.M. White. *Viscous fluid flow.* Mc Graw Hill, 1974.

[13] L. H. Wilke. *J. Math. Phys., 46-151*, 1967.